Table 4. The contribution of each polycyclic aromatic compound (PAC) to aryl hydrocarbon receptor (AhR) activity in airborne particulates by using the chemical-activated luciferase expression (CALUX) assay

Compound	IEF[a]	Concentration in aerosol[b] (ng/mg)	IEQ[c]	Contribution of each PAC[d]
Anthracene	NI[e]	1.6–0.8		
Phenanthrene	NI	24.3–13.9		
Fluoranthene	U[f]	45.0–21.4		
Pyrene	NI	52.5–25.8		
Benz[*a*]anthracene	0.26	23.9–12.2	6.2	0.083%
Chrysene	0.35	47.2–24.8[g]	17	0.23%
Triphenylene	U	47.2–24.8[g]		
Benzo[*b*]fluorine	0.046	6.0–3.4	0.28	0.0038%
Benzo[*b*]fluoranthene	4.7	71.5–17.7	336	4.5%
Benzo[*k*]fluoranthene	84	76.7–17.0	6,443	86%
Benzo[*a*]pyrene	1	33.9–7.9	34	0.46%
Dibenz[*a,h*]anthracene	9.0	41.9–3.7	377	5.1%
Indeno[1,2,3-*cd*]pyrene	2.5	87.9–11.9	220	3.0%
Benzo[*ghi*]perylene	U	193.4–28.4		
Phenalenone	<0.0027	183.6–93.8	0.50	0.0067%
7*H*-Benz[*de*]anthracen-7-one	U	87.4–53.7		
Fluorenone	NI	57.6–12.3		
Xanthone	NI	8.2–1.8		
11*H*-Benzo[*a*]fluoren-11-one	0.37	31.9–17.0	12	0.16%
11*H*-Benzo[*b*]fluoren-11-one	0.072	62.7–36.3	1.6	0.060%
Cyclopenta[*cd*]pyren-3(4*H*)-one	0.0038	2.4–2.2	0.0091	0.00012%
6*H*-Benzo[*cd*]pyren-6-one	U	134.2–65.9		
Anthraquinone	NI	31.9–12.9		
7,12-benz[*a*]anthracenequinone	0.028	39.9–14.0	1.1	0.015%
5,12-Naphthacenequinone	0.13	13.2–4.8	1.7	0.023%
Naphthalic anhydride	U	195.5		

[a] Induction equivalency factor (IEF) relative to benzo[*a*]pyrene (mouse hepatoma cell system).
[b] ng/mg equivalent organic carbon (1993, South California; data from Hannigan et al. [1]).
[c] Induction equivalent (IEQ) relative to benzo[*a*]pyrene (concentration multiplied by IEF). The maximum concentration in the mass concentration range of each compound was used for the calculation of IEQ.
[d] Percentage IEQ in the sum of calculated IEQs.
[e] NI = not induced.
[f] U = less than 25% of the maximal response to 2,3,7,8-tetrachlorodibenzo-*p*-dioxin (TCDD).
[g] This value is the sum of chrysene and triphenylene. The IEQ of chrysene is calculated by assuming this value as the total amount of chrysene.

Contribution ratio to the total AhR activity in environmental samples

The CALUX assay using H1L1 cells is more suitable than the yeast assay when comparing AhR ligand activity of individual compound for the evaluation of exposure effect to wildlife and humans, because compounds are thought to be absorbed and metabolized more easily in mammalian cells than in yeast cells and the handling of CALUX assay is simple (Table 1). By using the result of the CALUX assay and analytical data from other researchers, it was expected that in gasoline exhaust particulates [3], the contribution of B[*k*]FA in the total concentration of multiplied IEF of each PAC examined in this research (this is called induction equivalent [IEQ] relative to B[*a*]P) was very high (88%), followed by B[*b*]FA and IdP (4.9 and 2.3%, respectively) (Table 3) [6,12]. It was predicted that PAKs such as B[*a*]FO and B[*b*]FO occupied 1.3 and 0.26%, respectively, of the total, and each contribution matched the contribution of PAHs such as B[*a*]P, Chr, and B[*a*]A, in gasoline exhaust particulates (1.0, 1.2, and 0.80%, respectively) (Table 3) [1,3]. It also was expected that in airborne particulates [1], the contribution of several PAHs in the total IEQs of each PAC examined in the present research was high for B[*k*]FA, DB[*a,h*]A, B[*b*]FA, and IdP (86, 5.1, 4.5, and 3.0%, respectively) [6,12], and the contribution of PAKs such as B[*a*]FO and B[*b*]FO matched that of PAHs such as B[*a*]P, Chr, and B[*a*]A (0.16, 0.060, 0.46, 0.23, and 0.083%, respectively) (Table 4) [1]. Machala et al. [6] found that other five-ring PAHs, such as benzo[*j*]fluoranthene and dibenz[*a,j*]anthracene, also contributed, to some extent, to the total AhR activity in river sediments.

CONCLUSION

This manuscript proposed that the CALUX assay is more suitable for evaluation of AhR ligand activities of PACs than the yeast assay from experimental data. Reports about AhR activities of PAKs and PAQs are few, but in the present study, NCQ, BAQ, B[*a*]FO, and B[*b*]FO showed strong AhR activities. In addition, it is predicted that these compounds contribute, to some extent, to the total AhR activities of atmospheric environmental samples. It was predicted that PAKs such as B[*a*]FO and B[*b*]FO occupied 0.06 to 1.3%, of the total IEQs of each PAC examined in the present research, and each contribution matched the contribution of PAHs such as B[*a*]P, Chr, and B[*a*]A in gasoline exhaust particulates and airborne particulates using data from the CALUX assay.

Acknowledgement—We thank Charles A. Miller III of the Department of Environmental Health Sciences and the Tulane–Xavier Center for Bioenvironmental Research, Tulane University School of Public Health and Tropical Medicine (New Orleans, LA, USA), for kindly supplying us with the YCM3 strain and Robert Kanaly of the Department of Environmental Biosciences and the International Graduate School of Arts and Sciences, Yokohama City University (Yokohama, Japan) for help in manuscript preparation. This work was supported, in part, by Grants-in-aid for Scientific Research (13027245, 16201012) from the Japanese Ministry of Education, Science, Sports, and Culture.

REFERENCES

1. Hannigan MP, Cass GR, Penman BW, Crespi CL, Lafleur AL, Busby WF Jr, Thilly WG, Simoneit BRT. 1998. Bioassay-directed chemical analysis of Los Angeles airborne particulate matter using a human cell mutagenicity assay. *Environ Sci Technol* 32: 3502–3514.
2. Rogge WF, Hildemann LM, Mazurek MA, Cass GR. 1993. Sources of fine organic aerosol. 2. Noncatalyst and catalyst-equipped automobiles and heavy-duty diesel trucks. *Environ Sci Technol* 27:636–651.
3. Alsberg T, Strandell M, Westerholm R, Stenberg U. 1985. Fractionation and chemical analysis of gasoline exhaust particulate extracts in connection with biological testing. *Environ Int* 11: 249–257.
4. Yamashita N, Kannan K, Imagawa T, Villneuve DL, Hashimoto S, Miyazaki A, Giesy JP. 2000. Vertical profile of polychlorinated dibenzo-*p*-dioxins, dibenzofurans, naphthalenes, biphenyls, polycyclic aromatic hydrocarbons, and alkylphenols in a sediment core from Tokyo Bay, Japan. *Environ Sci Technol* 34:3560–3567.
5. Moore MN, Livingstone DR, Widdows J. 1989. Hydrocarbons in marine mollusks: Biological effects and ecological consequences. In Varanasi U, ed, *Metabolism of Polycyclic Aromatic Hydrocarbons in the Aquatic Environment.* CRC, Boca Raton, FL, USA, pp 291–328.
6. Machala M, Vondráček J, Bláha L, Ciganek M, Neča J. 2001. Aryl hydrocarbon receptor–mediated activity of mutagenic polycyclic aromatic hydrocarbons determined using in vitro reporter gene assay. *Mutat Res* 497:49–62.
7. Yoshida S, Sagai M, Oshio S, Umeda T, Ihara T, Sugamata M, Sugawara I, Takeda K. 1999. Exposure to diesel exhaust affects the male reproductive system of mice. *Int J Androl* 22:307–315.
8. Watanabe N, Oonuki Y. 1999. Inhalation of diesel engine exhaust affects spermatogenesis in growing male rats. *Environ Health Perspect* 107:539–544.
9. Okamura K, Kizu R, Toriba A, Murahashi T, Mizokami A, Burnstein KL, Klinge CM, Hayakawa K. 2004. Antiandrogenic activity of extracts of diesel exhaust particles emitted from diesel-engine truck under different engine loads and speeds. *Toxicology* 195: 243–254.
10. Kizu R, Okamura K, Toriba A, Kakishima H, Mizokami A, Burnstein KL, Hayakawa K. 2003. A role of aryl hydrocarbon receptor in the antiandrogenic effects of polycyclic aromatic hydrocarbons in LNCaP human prostate carcinoma cells. *Arch Toxicol* 77:335–343.
11. Ohtake F, Takeyama K, Matsumoto T, Kitagawa H, Yamamoto Y, Nohara K, Tohyama C, Krust A, Mimura J, Chambon P, Yanagisawa J, Fujii-Kuriyama Y, Kato S. 2003. Modulation of estrogen receptor signaling by association with the activated dioxin receptor. *Nature* 423:545–550.
12. Machala M, Ciganek M, Bláha L, Minksová K, Vondráček J. 2001. Aryl hydrocarbon receptor–mediated and estrogenic activities of oxygenated polycyclic aromatic hydrocarbons and azaarenes originally identified in extracts of river sediments. *Environ Toxicol Chem* 20:2736–2743.
13. Kamiya M, Toriba A, Onoda Y, Kizu R, Hayakawa K. 2005. Evaluation of estrogenic activities of hydroxylated polycyclic aromatic hydrocarbons in cigarette smoke condensate. *Food Chem Toxicol* 43:1017–1027.
14. Miller CA III. 1999. A human aryl hydrocarbon receptor signaling pathway constructed in yeast displays additive responses to ligand mixtures. *Toxicol Appl Pharmacol* 160:297–303.
15. Riddick DS, Huang Y, Harper PA, Okey AB. 1994. 2,3,7,8-Tetrachlorodibenzo-*p*-dioxin versus 3-methylcholanthrene: Comparative studies of Ah receptor binding, transformation, and induction of CYP1A1. *J Biol Chem* 269:12118–12128.
16. Ziccardi MH, Gardner IA, Denison MS. 2002. Application of the luciferase recombinant cell culture bioassay system for the analysis of polycyclic aromatic hydrocarbons. *Environ Toxicol Chem* 21:2027–2033.
17. Jones JM, Anderson JW. 1999. Relative potencies of PAHs and PCBs based on the response of human cells. *Environ Toxicol Pharmacol* 7:19–26.
18. Iwanari M, Nakajima M, Kizu R, Hayakawa K, Yokoi T. 2002. Induction of CYP1A1, CYP1A2, and CYP1B1 mRNAs by nitropolycyclic aromatic hydrocarbons in various human tissue–derived cells: Chemical-, cytochrome P450 isoform–, and cell-specific differences. *Arch Toxicol* 76:287–298.
19. Denison MS, Pandini A, Nagy SR, Baldwin EP, Bonati L. 2002. Ligand binding and activation of the Ah receptor. *Chem-Biol Interact* 141:3–24.
20. Adachi J, Mori Y, Matsui S, Matsuda T. 2004. Comparison of gene expression patterns between 2,3,7,8-tetrachlorodibenzo-*p*-dioxin and a natural aryl hydrocarbon receptor ligand, indirubin. *Toxicol Sci* 80:161–169.
21. Rannug U, Rannug A, Sjberg U, Li H, Westerholm R, Bergman J. 1995. Structure elucidation of two tryptophan-derived, high-affinity Ah receptor ligands. *Chem Biol* 2:841–845.
22. Amakura Y, Tsutsumi T, Nakamura M, Kitagawa H, Fujino J, Sasaki K, Toyoda M, Yoshida T, Maitani T. 2003. Activation of the aryl hydrocarbon receptor by some vegetable constituents determined using in vitro reporter gene assay. *Biol Pharm Bull* 26:532–539.
23. Møller M, Hagen I, Ramdahl T. 1985. Mutagenicity of polycyclic aromatic compounds (PAC) identified in source emissions and ambient air. *Mutat Res* 157:149–156.
24. Tada K, Odashima N, Ishidate M. 1966. On the screening experiment for the carcinogenesis of polycyclic quinones. *Kyoritsu Pharmaceutical University Environmental Document* 63–68.
25. Misaki K, Matsui S, Matsuda T. 2007. Metabolic enzyme induction by HepG2 cells exposed to oxygenated and nonoxygenated polycyclic aromatic hydrocarbons. *Chem Res Toxicol* 20:277–283.
26. Streitwieser A Jr, Brown SM. 1988. Convenient preparation of 11*H*-benzo[*a*]fluorenone and 11*H*-benzo[*b*]fluorenone. *J Org Chem* 53:904–906.
27. Fieser LF, Joshel LM. 1940. 9-Methyl-3,4-benzofluorene. *J Am Chem Soc* 62:957–958.
28. Spijker NM, van den Braken-van Leersum AM, Lugtenburg J, Cornelisse J. 1990. A very convenient synthesis of cyclopenta[*cd*]pyrene. *J Org Chem* 55:756–758.
29. Clar E, Mackay CC. 1972. Circobiphenyl and the attempted synthesis of 1:14-, 3:4-, 7:8-, 10:11-tetrabenzoperopyrene. *Tetrahedron* 28:6041–6047.
30. Sarna LP, Hudge PE, Webster GRB. 1984. Octanol–water partition coefficients of chlorinated dioxins and dibenzofurans by reversed-phase HPLC using several C_{18} columns. *Chemosphere* 13: 975–983.
31. Shiu WY, Doucett W, Gobas FAPC, Andren A, Mackay D. 1988. Physical–chemical properties of chlorinated dibenzo-*p*-dioxins. *Environ Sci Technol* 22:651–658.
32. Smith CJ, Hansch C. 2000. The relative toxicity of compounds in mainstream cigarette smoke condensate. *Food Chem Toxicol* 38:637–646.
33. Choi J, Oris JT. 2003. Assessment of the toxicity of anthracene photomodification products using the topminnow (*Poeciliopsis lucida*) hepatoma cell line (PLHC-1). *Aquat Toxicol* 65:243–251.
34. Eugster H-P, Sengstag C, Meyer UA, Hinnen A, Würgler FE. 1990. Constitutive and inducible expression of human cytochrome P450IA1 in yeast *Saccharomyces cerevisiae*: An alternative enzyme source for in vitro studies. *Biochem Biophys Res Commun* 172:737–744.
35. Ema M, Ohe N, Suzuki M, Mimura J, Sogawa K, Ikawa S, Fujii-Kuriyama Y. 1994. Dioxin binding activities of polymorphic forms of mouse and human aryl hydrocarbon receptors. *J Biol Chem* 269:27337–27343.
36. Kawanishi M, Sakamoto M, Ito A, Kishi K, Yagi T. 2003. Construction of reporter yeasts for mouse aryl hydrocarbon receptor ligand activity. *Mutat Res* 540:99–105.
37. Cox MB, Miller CA III. 2004. Cooperation of heat shock protein 90 and p23 in aryl hydrocarbon receptor signaling. *Cell Stress Chaperons* 9:4–20.
38. Garrison PM, Tullis K, Aarts JMMJG, Brouwer A, Giesy JP, Denison MS. 1996. Species-specific recombinant cell lines as bioassay systems for the detection of 2,3,7,8-tetrachlorodibenzo-*p*-dioxin-like chemicals. *Fundam Appl Toxicol* 30:194–203.
39. Han D, Nagy SR, Denison MS. 2004. Comparison of recombinant cell bioassays for the detection of Ah receptor agonists. *BioFactors* 20:11–22.
40. Rannug U, Sjgren M, Rannug A, Gillner M, Toftgård R, Gustafsson J-Å, Rosenkranz H, Klopman G. 1991. Use of artificial intelligence in structure-affinity correlations of 2,3,7,8-tetrachlorodibenzo-*p*-dioxin (TCDD) receptor ligands. *Carcinogenesis* 12: 2007–2015.

Carcinogenesis vol.28 no.11 pp.2363–2366, 2007
doi:10.1093/carcin/bgm057
Advance Access publication March 14, 2007

Increased formation of hepatic N^2-ethylidene-2′-deoxyguanosine DNA adducts in *aldehyde dehydrogenase 2*-knockout mice treated with ethanol

Tomonari Matsuda*, Akiko Matsumoto[1], Mitsuhiro Uchida, Robert A. Kanaly[2], Kentaro Misaki, Shinya Shibutani[3], Toshihiro Kawamoto[4], Kyoko Kitagawa[5], Keiichi I.Nakayama[6], Katsumaro Tomokuni[1] and Masayoshi Ichiba[1]

Graduate School of Global Environmental Studies, Kyoto University, Kyoto 606-8501, Japan, [1]Department of Social and Environmental Medicine, Saga Medical School, Saga 849-8501, Japan, [2]Department of Environmental Biosciences, Yokohama City University, Yokohama, Kanagawa 236-0027, Japan, [3]Department of Pharmacological Sciences, State University of New York at Stony Brook, Stony Brook, NY 11794-8651, USA, [4]Department of Environmental Health, University of Occupational and Environmental Health, Kitakyusyu, Fukuoka 807-8555, Japan, [5]First Department of Biochemistry, Hamamatsu University School of Medicine, Hamamatsu, Shizuoka 431-3192, Japan and [6]Department of Molecular and Cellular Biology, Medical Institute of Bioregulation, Kyusyu University, Fukuoka 812-8582, Japan

*To whom correspondence should be addressed. Tel: +75 753 5052
Fax: +81 75 753 3335;
Email: matsuda@eden.env.kyoto-u.ac.jp
Correspondence may also be addressed to Masayoshi Ichiba.
Fax: +81 952 34 2065;
Email: ichiba@cc.saga-u.ac.jp

N^2-ethylidene-2′-deoxyguanosine (N^2-ethylidene-dG) is a major DNA adduct induced by acetaldehyde. Although it is unstable in the nucleoside form, it is relatively stable when present in DNA. In this study, we analyzed three acetaldehyde-derived DNA adducts, N^2-ethylidene-dG, N^2-ethyl-2′-deoxyguanosine (N^2-Et-dG) and α-methyl-γ-hydroxy-1,N^2-propano-2′-deoxyguanosine (α-Me-γ-OH-PdG) in the liver DNA of *aldehyde dehydrogenase* (*Aldh*)-2-knockout mice to determine the influence of alcohol consumption and the *Aldh2* genotype on the levels of DNA damage. In control *Aldh2*+/+ mice, the level of N^2-ethylidene-dG adduct in liver DNA was 1.9 ± 0.7 adducts per 10^7 bases and was not significantly different than that of *Aldh2*+/− and −/− mice. In alcohol-fed mice (20% ethanol for 5 weeks), the adduct levels of *Aldh2*+/+, +/− and −/− mice were 7.9 ± 1.8, 23.3 ± 4.0 and 79.9 ± 14.2 adducts per 10^7 bases, respectively, and indicated that adduct level was alcohol and Aldh2 genotype dependent. In contrast, an alcohol- or *Aldh2* genotype-dependent increase was not observed for α-Me-γ-OH-PdG, and N^2-Et-dG was not detected in any of the analyzed samples. In conclusion, the risk of formation of N^2-ethylidene-dG in model animal liver *in vivo* is significantly higher in the *Aldh2*-deficient population and these results may contribute to our understanding of *in vivo* adduct formation in humans.

Introduction

Alcohol consumption is a risk factor for hepatocellular carcinoma and acetaldehyde, a carcinogenic intermediate of ethanol, has been suggested to be involved in the occurrence of hepatocellular carcinoma. Two large-scale epidemiological studies revealed that habitual alcohol drinking was probably lead to an increased risk of hepatocellular carcinoma and that a lack of acetaldehyde-metabolizing enzyme activity [aldehyde dehydrogenase (ALDH)-2] was associated with this increased risk (1,2).

There are several enzymes responsible for metabolizing alcohol in the liver. The first step is oxidization of ethanol to acetaldehyde by alcohol dehydrogenase (ADH) and the ADH holoenzyme may exist as either a homodimer or heterodimer of α, β and γ subunits, encoded by *ADH1*, *ADH2* and *ADH3*, respectively. The second step is oxidation of acetaldehyde to acetic acid by ALDH or inducible cytochrome P450 2E1. Human ALDH isozymes are divided into two groups determined by their Michaelis constant values for acetaldehyde: the low K_m ALDH (ALDH1 and ALDH2) and high K_m ALDH (ALDH3 and ALDH4). The K_m values of ALDH3 and ALDH4 are on the order of millimolar (5–83 mM) (3), cytosolic ALDH1 is on the order of micromolar (180 μM) and mitochondrial ALDH2 is on the order of nanomolar (200 nM) (4), suggesting that ALDH2 is a key enzyme responsible for catalyzing oxidation acetaldehyde in human liver. Approximately 40% of Japanese have a mutation in the *ALDH2* gene whereas most Caucasians and Africans do not (5). ALDH2 is a homotetrameric enzyme and the mutant *ALDH2*2* allele (Glu487Lys) encodes for a catalytically inactive subunit (6). It is predicted that individuals who possess the *ALDH2*1/2*2* genotype will have only 6.25% of the normal ALDH2 protein and that other tetramers containing one or more of the ALDH2*2 subunits are mostly inactive. However, when taken together, the overall measured activity of the five possible tetramer combinations of the *ALDH2*1/2*2* genotype is ~13% (7,8). Lastly, individuals who are *ALDH2*2/2*2* homozygous have little ALDH2 activity.

Acetaldehyde itself is a carcinogen that induced nasal tumors in experimental animals by inhalation (9), and is thought to be a tumor initiator because of its mutagenic and DNA-damaging properties (10–13). Recently, we developed an analytical method for acetaldehyde-derived stable DNA adducts, N^2-ethyl-2′-deoxyguanosine (N^2-Et-dG), α-*S*- and α-*R*-methyl-γ-hydroxy-1,N^2-propano-2′-deoxyguanosine (α-*S*-Me-γ-OH-PdG and α-*R*-Me-γ-OH-PdG) by using sensitive liquid chromatography tandem mass spectrometry (LC/MS/MS) (14). Other than these stable DNA adducts, the reaction of acetaldehyde with deoxyguanosine results in the formation of an unstable Schiff base at the N^2 position of deoxyguanosine [N^2-ethylidene-2′-deoxyguanosine (N^2-ethylidene-dG)] (Figure 1). Wang *et al.* (15) showed that N^2-ethylidene-dG in human liver DNA is relatively stable and that the presence of this adduct could be confirmed by detection of N^2-Et-dG after reduction of DNA during isolation and enzymatic hydrolysis. They showed that when the reduction step was included during these steps that approximately a few 100 times more N^2-Et-dG was detected in some cases. In this study, we analyzed these acetaldehyde-derived DNA adducts in the liver DNA of *Aldh2*-knockout mice that were exposed to alcohol to determine the effects of alcohol consumption and the *Aldh2* genotype on the levels of DNA damage in the target organ.

Abbreviations: ADH, alcohol dehydrogenase; ALDH, aldehyde dehydrogenase; εdA, 1,N^6-etheno-2′-deoxyadenosine; LC/MS/MS, liquid chromatography tandem mass spectrometry; α-Me-γ-OH-PdG, α-methyl-γ-hydroxy-1, N^2-propano-2′-deoxyguanosine; N^2-Et-dG, N^2-ethyl-2′-deoxyguanosine; N^2-ethylidene-dG, N^2-ethylidene-2′-deoxyguanosine.

Materials and methods

Aldh2-knockout mice

Aldh2-knockout mice, which had been backcrossed with C57BL6, were obtained from the Department of Environmental Health, University of Occupational and Environmental Health, Japan. Male mice, aged 10–11 weeks old, were used in conformity with the regulations of the committee on animal experiments of Saga University, Japan. The genomic DNA of all subjects was extracted twice—from a small part of the ear and the lung—and the genotype of Aldh2 was determined by polymerase chain reaction according to the method of Kitagawa *et al.* (16).

Alcohol feeding

Male mice were fed an ethanol solution (20%) and standard hard feed CR-LPF (348 kcal/100 g) (Charles River Japan, Yokohama, Japan) for 5 weeks. The number of mice ranged from four to six per group. After 5 weeks, the mice were killed and liver tissue specimens were removed immediately after blood collection, and then parts of the tissue specimens were frozen in liquid nitrogen and stored at −80°C until they were analyzed.

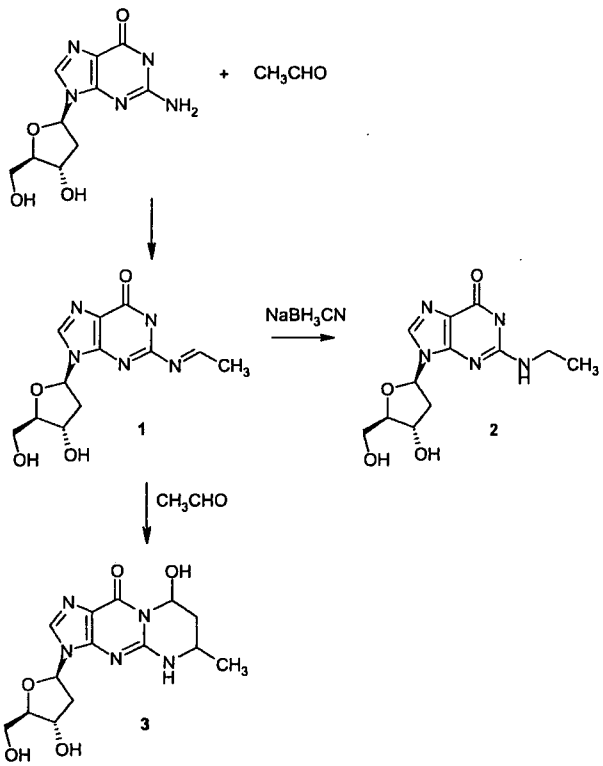

Fig. 1. Formation of acetaldehyde–deoxyguanosine adducts. **1**, N^2-ethylidene-dG; **2**, N^2-Et-dG and **3**, α-Me-γ-OH-PdG.

DNA isolation from mouse liver

For quantification of N^2-Et-dG, α-methyl-γ-hydroxy-1,N^2-propano-2′-deoxyguanosine (α-Me-γ-OH-PdG) and 1,N^6-etheno-2′-deoxyadenosine (εdA), DNA was purified from mouse liver (~50 mg amounts) by using Puregene™ DNA Purification System Cell and Tissue kit. The protocol was performed basically as described according to the manufacturer except that desferroxamine (final concentration: 0.1 mM) was added to all solutions to avoid formation of oxidative adducts during the purification step.

For quantification of N^2-ethylidene-dG, DNA was isolated from mouse liver (~50 mg amounts) as described by Wang *et al.* (15). The Puregene™ DNA Purification System Cell and Tissue kit was used. The protocol was basically as described according to the manufacturer except that $NaBH_3CN$ was added to the Puregene cell lysis solution (final concentration was 150 mM) and other solutions (2-propanol, Tris–ethylenediaminetetraacetic acid, ethanol and 70% ethanol; final concentration was 100 mM). After the purification step, DNA was dissolved in 10 mM Tris–HCl/5 mM ethylenediaminetetraacetic acid buffer (pH 7), extracted with chloroform and precipitated with ethanol also as described by Wang *et al.* (15).

DNA adduct standards and their stable isotopes

N^2-Et-dG, α-Me-γ-OH-PdG and their [U-$^{15}N_5$]-labeled standards were synthesized as described previously (14). εdA was purchased from Sigma-Aldrich Japan, Tokyo, Japan and [U-$^{15}N_5$] εdA was prepared from [U-$^{15}N_5$] dA (Cambridge Isotope Laboratory, Andover, MA, USA) following a method as described previously (17).

DNA digestion

DNA samples (20 μg) were digested to their corresponding 2′-deoxyribonucleoside-3′-monophosphates by the addition of 15 μl of 17 mM citrate plus 8 mM $CaCl_2$ buffer that contained micrococcal nuclease (22.5 U) and spleen phosphodiesterase (0.075 U) plus internal standards. Solutions were mixed and incubated for 3 h at 37°C, after which alkaline phosphatase (3 U), 10 μl of 0.5 M Tris–HCl (pH 8.5), 5 μl of 20 mM $ZnSO_4$ and 67 μl of distilled water were added and incubated further for 3 h at 37°C. The digested sample was extracted twice with methanol. The methanol fractions were evaporated to dryness, resuspended in 100 μl of distilled water and subjected to LC/MS/MS.

Instrumentation

LC/MS/MS analyses were performed using a Shimadzu LC system (Shimadzu, Kyoto, Japan) interfaced with a Quattro Ultima triple stage quadrupole MS (Waters–Micromass, Manchester, UK). The LC column was eluted over a gradient that began at a ratio of 2% methanol to 98% water and was changed to 40% methanol over a period of 40 min, changed to 80% methanol from 40 to 45 min and finally returned to the original starting conditions, 2:98, for the remaining 15 min. The total run time was 60 min. Sample injection volumes of 50 μl each were separated on a Shim-pack FC-ODS column (4.6 × 150 mm; Shimadzu) and eluted at a flow rate of 0.4 ml/min. Mass spectral analyses were carried out in positive ion mode with nitrogen as the nebulizing gas. The ion source temperature was 130°C, the desolvation gas temperature was 380°C and the cone voltage was operated at a constant 35 V. Nitrogen gas was also used as the desolvation gas (700 l/h) and cone gas (35 l/h) and argon was used as the collision gas at a collision cell pressure of 1.5×10^{-3} mbar. Positive ions were acquired in multiple reaction monitoring (MRM) mode. The MRM transitions monitored were as follows: [$^{15}N_5$]-α-Me-γ-OH-PdG, *m/z* 343 → 227; α-Me-γ-OH-PdG, *m/z* 338 → 222; [$^{15}N_5$]-N^2-Et-dG, *m/z* 301 → 185; N^2-Et-dG, *m/z* 296 → 180; [$^{15}N_5$]-εdA, *m/z* 281 → 165 and εdA, *m/z* 276 → 160. The amount of each DNA adduct was quantified by the ratio of the peak area of the target adducts and of its stable isotope. QuanLynx (version 4.0) software (Waters–Micromass) was used to create standard curves and to calculate the adduct concentrations. The amount of deoxyguanosine was monitored by a Shimadzu SPD-10A UV-Visible detector that was in place before the tandem MS.

Results

Ethanol and food intake by male mice

The male mice were fed with water or 20% ethanol and standard hard feed for 5 weeks. Feed intake was slightly decreased in the 20% ethanol group, but not significantly different between *Aldh2* genotypes. The average ethanol intake in the case of the 20% ethanol group was not significantly different between *Aldh2* genotypes (~23 g/day/kg body wt) whereas significant losses in body weight were observed only in the *Aldh2−/−* mice (data not shown).

DNA adduct levels in the liver of control and alcohol-treated mice

After 5 weeks, mice were killed and their liver DNA was purified to detect DNA adduct levels. The acetaldehyde-inducible stable DNA adducts, N^2-Et-dG and α-Me-γ-OH-PdG, were analyzed and εdA, a DNA adduct induced by lipid peroxidation, was also analyzed for comparative purposes. The LC/MS/MS instrument employed for analyzing these adducts was sensitive enough to detect at least one adduct per 10^8 bases in this experimental protocol (14). However, N^2-Et-dG was not detected in any liver DNA samples for both alcohol-treated and non-treated mice for any *Aldh2* genotype. α-Me-γ-OH-PdG and εdA were detected in all the samples analyzed but neither alcohol-dependent nor Aldh2 genotype-dependent increases in adduct levels were observed (Figure 2).

Detection of hepatic N^2-ethylidene-dG adduct in Aldh2-knockout mice

To measure N^2-ethylidene-dG in DNA, liver samples were homogenized in lysis buffer containing the strong reducing agent $NaBH_3CN$, followed by DNA purification in the presence of $NaBH_3CN$. During the purification step, it was expected that N^2-ethylidene-dG would be converted to stable N^2-Et-dG. The average N^2-ethylidene-dG level in liver DNA from untreated *Aldh2+/+* mice was 1.9 ± 0.7 adducts per 10^7 bases. Both *Aldh2* hetero- and homo-deficient genotypes did not affect N^2-ethylidene-dG levels in untreated mice. However, in the 20% ethanol-consuming mice, significant increases in the levels of N^2-ethylidene-dG in the liver DNA of *Aldh2+/+* mice (7.9 ± 1.8 adducts per 10^7 bases) and *Aldh2+/−* and *Aldh2−/−* mice were observed; levels were 23.3 ± 4.0 and 79.9 ± 14.2 adducts per 10^7 bases in *Aldh2+/−* and *Aldh2−/−* mouse liver DNA, respectively (Figure 3). These data indicated an *Aldh2* genotype-dependent increase in the levels of N^2-ethylidene-dG in liver DNA.

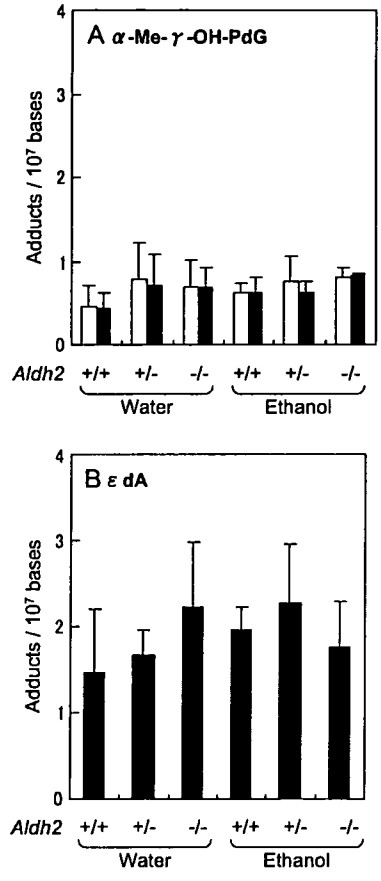

Fig. 2. DNA adduct levels in control and alcohol-treated mice having different *Aldh2* genotypes. Mice were fed with water (*Aldh2*+/+: $n = 5$, +/−: $n = 7$ and −/−: $n = 5$) or 20% ethanol (*Aldh2*+/+: $n = 6$, +/−: $n = 5$ and −/−: $n = 2$) for 5 weeks. Liver DNA samples were purified without addition of reducing agent $NaBH_3CN$. (**A**) The levels of α-Me-γ-OH-PdG (open bar: α-*S*-Me-γ-OH-PdG and closed bar: α-*R*-Me-γ-OH-PdG). (**B**) The levels of εdA. The error bars represent the standard deviation.

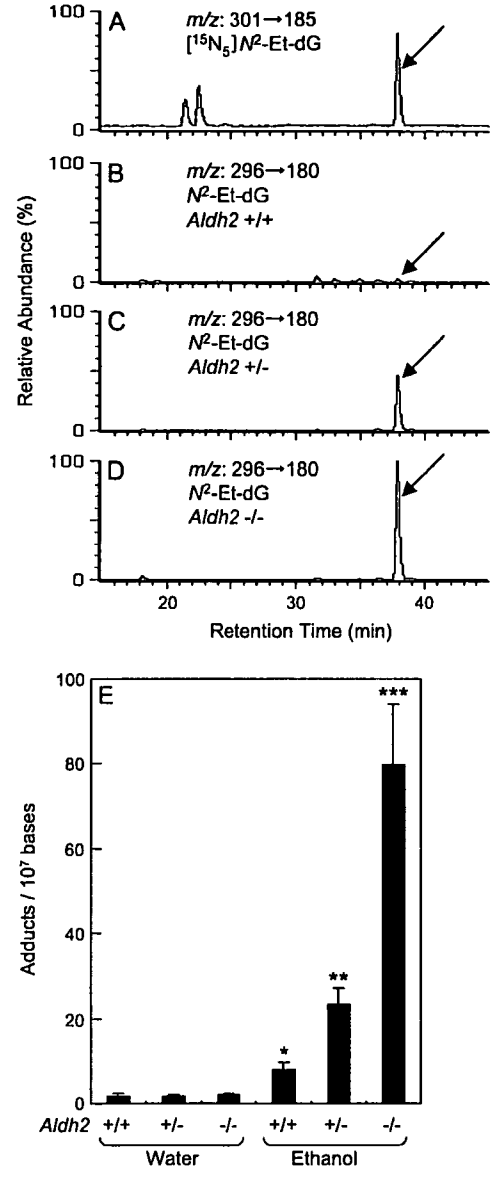

Fig. 3. Alcohol- and *Aldh2* genotype-dependent increases in N^2-ethylidene-dG levels in mice liver DNA. Mice with various *Aldh2* genotypes were fed with water (*Aldh2*+/+: $n = 5$, +/−: $n = 7$ and −/−: $n = 5$) or 20% ethanol (*Aldh2*+/+: $n = 6$, +/−: $n = 5$ and −/−: $n = 4$) for 5 weeks and the liver DNA was purified under the presence of $NaBH_3CN$ to reduce unstable N^2-ethylidene-dG to stable N^2-Et-dG. N^2-ethylidene-dG was detected as N^2-Et-dG by using LC/MS/MS. (**A**) A representative LC/MS/MS chromatogram of transition *m/z* 301 → 185 for [U-$^{15}N_5$] N^2-Et-dG as an internal standard. (**B–D**) Representative LC/MS/MS chromatograms of transition *m/z* 296 → 180 for N^2-Et-dG in *Aldh2*+/+ (**B**), +/− (**C**) and −/− (**D**) mice. (**E**) The levels of N^2-ethylidene-dG in mice liver DNA. The error bars represent the standard deviation. *Significantly increased from water control (+/+); **significantly increased from water control (+/−) or ethanol-treated *Aldh2*+/+ mice and ***significantly increased from water control (−/−) or ethanol-treated *Aldh2*+/+ and +/− mice ($P < 0.01$).

Discussion

The ALDH2-knockout mouse developed by Kitagawa *et al.* (16) has a portion of the phosphoglycerate kinase (PGK) gene promoter containing an in frame termination codon inserted immediately downstream of exon 3. The *Aldh2*−/− mouse has null mRNA of *Aldh2*, null ALDH2 protein and null mitochondrial aldehyde oxidation activity in the liver, but maintains a normal level of cytosolic aldehyde oxidation activity. In the mouse model, no ALDH2 protein is expressed from the *Aldh2*-knockout gene due to the stop codon present in the inserted PGK promoter gene. In the *Aldh2*+/− mice liver, half of the activity for metabolizing acetaldehyde remains compared with the *Aldh2*+/+ mouse. On the other hand, human *ALDH2*1/2*2* heterozygotes have only 13% of the native activity because the heterotetramers of the *ALDH2*1* and *ALDH2*2* subunits do not function properly (8). Thus, ALDH2 activity in a human *ALDH2*2/2*1* heterozygote corresponds with that of the homozygous knockout (*Aldh2*−/−) mouse rather than the heterozygous (*Aldh2*+/−) mice.

Isse *et al.* (18) reported that the blood acetaldehyde concentration after gavage of ethanol (1 g/kg body wt) of *Aldh2*−/− mice was ~18 μM and that was 9.3 times higher than that of *Aldh2*+/+ mice. Our observations show that the N^2-ethylidene-dG levels in the liver DNA of the ethanol-fed *Aldh2*−/− mice was 10 times higher than that of *Aldh2*+/+ mice, and these data are consistent with data of acetaldehyde burden. Human alcohol challenge tests have shown that after drinking a moderate amount of ethanol (0.8 g/kg body wt), the average peak in blood acetaldehyde concentrations in *ALDH2*1/2*2* individuals was 23 μM and that was 7.5 times greater than that of active *ALDH2*1/2*1* homozygotes (19). Thus, it is possible that higher

N^2-ethylidene-dG levels in liver DNA exist in drinkers having *ALDH2*1/2*2* genotypes more than in *ALDH2*1/2*1* genotypes.

On the other hand, N^2-Et-dG, a reduced product of N^2-ethylidene-dG, was not detected in any of the liver DNA samples analyzed. Since our LC/MS/MS method can detect at least one N^2-Et-dG adduct in 10^8 nucleotides, the adduct level should be at least 18–800 times lower than in the case of N^2-ethylidene-dG in mouse liver DNA. α-Me-γ-OH-PdG, another acetaldehyde-induced DNA adduct, was detected at the level of 4.5–8.1 adducts per 10^8 nucleotides, however, neither significant alcohol-dependent nor *Aldh2* genotype-dependent increases in adduct levels were observed. Previously, we determined the DNA adducts in the blood of 44 DNA samples from Japanese alcoholic patients who consumed an average of 116 g of ethanol every day for 25 years, and the levels of N^2-Et-dG and α-Me-γ-OH-PdG were significantly higher in alcoholics with the *ALDH2*1/2*2* genotype as compared with those with the *ALDH2*1/2*1* genotype (14). Since many lymphoid cells are long-lived and may persist as memory cells for several years (20), N^2-Et-dG may accumulate in the lymphoid cells of such subjects. In this study, mice were fed alcohol for only 5 weeks and that may not have been enough time for these adducts to accumulate to detectable levels in the liver, although we should consider species-specific differences and tissue-specific differences with respect to endogenous reduction of N^2-ethylidene-dG and DNA repair activity. From our data in this study at least, we can clearly say that N^2-ethylidene-dG, rather than N^2-Et-dG and α-Me-γ-OH-PdG, is a sensitive biomarker for acetaldehyde exposure *in vivo*.

There have been several studies in regard to the mutagenicity of N^2-Et-dG and α-Me-γ-OH-PdG. N^2-Et-dG adducts induce G to C mutations during DNA synthesis catalyzed by the *Escherichia coli* DNA polymerase I Klenow fragment (21) and G to T mutations during gap-filling DNA synthesis in *E.coli* cells (22). N^2-ethyl-2′-deoxyguanosine triphosphate (N^2-Et-dGTP) was effectively utilized during DNA synthesis catalyzed by mammalian DNA polymerases α and δ (23). Additionally, it has been shown that N^2-Et-dG strongly blocks replicative DNA polymerization, which leads to frameshift deletion mutations (24,25). When a single-strand shuttle vector containing a single diastereoisomer of α-Me-γ-OH-PdG was propagated in a mammalian cell line, the mutational frequency was 5–6%; G to T transversions were detected as the dominant form of damage (26). In addition, α-Me-γ-OH-PdG adducts are thought to be the precursor lesions to DNA–DNA or DNA–protein cross-links (27,28). Taken together, these observations suggest that N^2-Et-dG and α-Me-γ-OH-PdG adducts are mutagenic DNA lesions that may cause human cancers, however, in regard to N^2-ethylidene-dG, little information is yet available about its biological significance.

In closing, although the biological significance of N^2-ethylidene-dG is not clear, it was clearly shown that the adduct levels in liver DNA were relatively high and significantly increased after alcohol uptake. It will be essential to study the mutagenicity and repair properties of this sensitive and abundant alcohol- and *Aldh2* genotype-dependent biomarker in the near future.

Acknowledgements

This research was supported in part by Grants-in-aid for Cancer Research from the Ministry of Health, Labor and Welfare of Japan and Grants-in-aid for Scientific Research from the Ministry of Education, Culture, Sports, Science and Technology of Japan.

Conflict of Interest Statement: None declared.

References

1. Munaka,M. *et al.* (2003) Genetic polymorphisms of tobacco- and alcohol-related metabolizing enzymes and the risk of hepatocellular carcinoma. *J. Cancer Res. Clin. Oncol.*, **129**, 355–360.
2. Sakamoto,T. *et al.* (2006) Influence of alcohol consumption and gene polymorphisms of *ADH2* and *ALDH2* on hepatocellular carcinoma in a Japanese population. *Int. J. Cancer*, **118**, 1501–1507.
3. Bosron,W.F. *et al.* (1987) Catalytic properties of human liver alcohol dehydrogenase isoenzymes. *Enzyme*, **37**, 19–28.
4. Klyosov,A.A. *et al.* (1996) Possible role of liver cytosolic and mitochondrial aldehyde dehydrogenases in acetaldehyde metabolism. *Biochemistry*, **35**, 4445–4456.
5. Goedde,H.W. *et al.* (1992) Distribution of *ADH2* and *ALDH2* genotypes in different populations. *Hum. Genet.*, **88**, 344–346.
6. Yoshida,A. *et al.* (1991) Genetics of human alcohol-metabolizing enzymes. *Prog. Nucleic Acids Res. Mol. Biol.*, **40**, 255–287.
7. Crabb,D.W. *et al.* (1989) Genotypes for aldehyde dehydrogenase deficiency and alcohol sensitivity: the inactive *ALDH2(2)* allele is dominant. *J. Clin. Invest.*, **83**, 314–316.
8. Wang,X. *et al.* (1996) Heterotetramers of human liver mitochondrial (class 2) aldehyde dehydrogenase expressed in *Escherichia coli*. A model to study the heterotetramers expected to be found in Oriental people. *J. Biol. Chem.*, **271**, 31172–31178.
9. International Agency for Research on Cancer. (1985) Allyl compounds, aldehydes, epoxides and peroxides. *IARC Monographs on the Evaluation of the Carcinogenic Risks to Humans*, **Vol. 36.** IARC, Lyon, pp. 101–132.
10. Wang,M. *et al.* (2000) Identification of DNA adducts of acetaldehyde. *Chem. Res. Toxicol.*, **13**, 1149–1157.
11. Matsuda,T. *et al.* (1998) Specific tandem GG to TT base substitutions induced by acetaldehyde are due to intra-strand crosslinks between adjacent guanine bases. *Nucleic Acids Res.*, **26**, 1769–1774.
12. Brooks,P.J. *et al.* (2005) DNA adducts from acetaldehyde: implications for alcohol-related carcinogenesis. *Alcohol*, **35**, 187–193.
13. Fang,J.L. *et al.* (1997) Detection of DNA adducts of acetaldehyde in peripheral white blood cells of alcohol abusers. *Carcinogenesis*, **18**, 627–632.
14. Matsuda,T. *et al.* (2006) Increased DNA damage in ALDH2-deficient alcoholics. *Chem. Res. Toxicol.*, **19**, 1374–1378.
15. Wang,M. *et al.* (2006) Identification of an acetaldehyde adduct in human liver DNA and quantitation as N^2-ethyldeoxyguanosine. *Chem. Res. Toxicol.*, **19**, 319–324.
16. Kitagawa,K. *et al.* (2000) Aldehyde dehydrogenase (ALDH) 2 associates with oxidation of methoxyacetaldehyde; *in vitro* analysis with liver subcellular fraction derived from human and *Aldh2* gene targeting mouse. *FEBS Lett.*, **476**, 306–311.
17. Hillestrom,P.R. *et al.* (2004) Quantification of 1,N^6-etheno-2′-deoxyadenosine in human urine by column-switching LC/APCI-MS/MS. *Free Radic. Biol. Med.*, **36**, 1383–1392.
18. Isse,T. *et al.* (2005) Aldehyde dehydrogenase 2 gene targeting mouse lacking enzyme activity shows high acetaldehyde level in blood, brain, and liver after ethanol gavages. *Alcohol. Clin. Exp. Res.*, **29**, 1959–1964.
19. Enomoto,N. *et al.* (1991) Acetaldehyde metabolism in different aldehyde dehydrogenase-2 genotypes. *Alcohol. Clin. Exp. Res.*, **15**, 141–144.
20. Roitt,I. *et al.* (1989) *Immunology*, 2nd edn. Gower Medical Publishing, London, 2.2.
21. Terashima,I. *et al.* (2001) Miscoding potential of the N^2-ethyl-2′-deoxyguanosine DNA adduct by the exonuclease free Klenow fragment of *Escherichia coli* DNA polymerase I. *Biochemistry*, **40**, 4106–4114.
22. Upton,D.C. *et al.* (2006) Mutagenesis by exocyclic alkylamino purine adducts in *Escherichia coli*. *Mutat. Res.*, **599**, 1–10.
23. Matsuda,T. *et al.* (1999) Effective utilization of N^2-ethyl-2′-deoxyguanosine triphosphate during DNA synthesis catalyzed by mammalian replicative DNA polymerases. *Biochemistry*, **38**, 929–935.
24. Perrino,F.W. *et al.* (2003) The N^2-ethylguanine and the O^6-ethyl-and O^6-methylguanine lesions in DNA: contrasting responses form the "bypass" DNA polymerase η and the replicative DNA polymerase α. *Chem. Res. Toxicol.*, **16**, 1616–1623.
25. Upton,D.C. *et al.* (2006) Replication of N^2-ethyldeoxyguanosine DNA adducts in the human embryonic kidney cell line 293. *Chem. Res. Toxicol.*, **19**, 960–967.
26. Fernandes,P.H. *et al.* (2005) Mammalian cell mutagenesis of the DNA adducts of vinyl chloride and crotonaldehyde. *Environ. Mol. Mutagen.*, **45**, 455–459.
27. Kozekov,I.D. *et al.* (2003) DNA interchain cross-links formed by acrolein and crotonaldehyde. *J. Am. Chem. Soc.*, **125**, 50–61.
28. Kurtz,A.J. *et al.* (2003) 1, N^2-Deoxyguanosine adducts of acrolein, crotonaldehyde, and trans-4-hydroxynonenal cross-link to peptides via Schiff base linkage. *J. Biol. Chem.*, **278**, 5970–5976.

Received November 13, 2006; revised February 22, 2007; accepted March 2, 2007

Available online at www.sciencedirect.com
ScienceDirect
Mutation Research 625 (2007) 83–93
Fundamental and Molecular Mechanisms of Mutagenesis
www.elsevier.com/locate/molmut
Community address: www.elsevier.com/locate/mutres

Application of the adductome approach to assess intertissue DNA damage variations in human lung and esophagus

Robert A. Kanaly [a,b], Saburo Matsui [a], Tomoyuki Hanaoka [c], Tomonari Matsuda [a,*]

[a] *Department of Technology and Ecology, Graduate School of Global Environmental Studies, Kyoto University, Kyoto 606-8501, Japan*
[b] *Department of Environmental Biosciences, International Graduate School of Arts and Sciences, Yokohama City University, Yokohama 236-0027, Japan*
[c] *Epidemiology and Prevention Division, National Cancer Center Research Institute, Tokyo 104-0045, Japan*

Received 28 February 2007; received in revised form 9 May 2007; accepted 14 May 2007
Available online 21 May 2007

Abstract

Methods for determining the differential susceptibility of human organs to DNA damage have not yet been explored to any large extent due to technical constraints. The development of comprehensive analytical approaches by which to detect intertissue variations in DNA damage susceptibility may advance our understanding of the roles of DNA adducts in cancer etiology and as exposure biomarkers at least. A strategy designed for the detection and comparison of multiple DNA adducts from different tissue samples was applied to assess esophageal and peripherally- and centrally-located lung tissue DNA obtained from the same person. This adductome approach utilized LC/ESI-MS/MS analysis methods designed to detect the neutral loss of 2′-deoxyribose from positively ionized 2′-deoxynucleoside adducts transmitting the $[M+H]^+ > [M+H-116]^+$ transition over 374 transitions. In the final analyses, adductome maps were produced which facilitated the visualization of putative DNA adducts and their relative levels of occurrence and allowed for comprehensive comparisons between samples, including a calf thymus DNA negative control. The largest putative adducts were distributed similarly across the samples, however, differences in the relative amounts of putative adducts in lung and esophagus tissue were also revealed. The largest-occurring lung tissue DNA putative adducts were 90% similar ($n = 50$), while putative adducts in esophagus tissue DNA were shown to be 80 and 84% similar to central and peripheral lung tissue DNA respectively. Seven DNA adducts, N^2-ethyl-2′-deoxyguanosine (N^2-ethyl-dG), 1,N^6-etheno-2′-deoxyadenosine (εdA), α-*S*- and α-*R*-methyl-γ-hydroxy-1,N^2-propano-2′-deoxyguanosine (1,N^2-PdG$_1$, 1,N^2-PdG$_2$), 3-(2′-deoxyribosyl)-5,6,7,8-tetrahydro-8-hydroxy-pyrimido[1,2-*a*]purine-(3*H*)-one (8-OH-PdG) and the two stereoisomers of 3-(2′-deoxyribosyl)-5,6,7,8-tetrahydro-6-hydroxypyrimido[1,2-*a*]purine-(3*H*)-one (6-OH-PdG) were unambiguously detected in all tissue DNA samples by comparison to authentic adduct standards and stable isotope dilution and their identities were matched to putative adducts detected in the adductome maps.

Keywords: DNA adduct; Intertissue variation; Adductome; Stable isotope dilution; Esophagus; Lung

1. Introduction

Xenobiotics from the environment and endogenously-produced oxidants may damage DNA by the production of DNA adducts and this vulnerability of cellular DNA to modification occurs continuously [1,2]. Consid-

* Corresponding author. Tel.: +81 75 753 5171; fax: +81 75 753 3335.
E-mail address: matsuda@z05.mbox.media.kyoto-u.ac.jp (T. Matsuda).

0027-5107/$ – see front matter © 2007 Elsevier B.V. All rights reserved.
doi:10.1016/j.mrfmmm.2007.05.006

ering that the initiating event in chemical carcinogenesis is the binding of a reactive compound to DNA to form a DNA adduct, DNA adducts have become the focus of intensive research over the last 30 years and are the subject of recent excellent reviews [3–8]. Generally, DNA adducts are repaired with high efficiency in the cells of the body, however, when adducts are unrepaired or misrepaired they may result in a variety of potentially deleterious consequences such as mutagenesis, carcinogenesis, accelerated aging or neurological syndromes such as Alzheimer's disease. To understand more clearly the roles of DNA adducts in (1) the etiology of these processes, (2) as biomarkers of exposure and (3) as potential markers of cancer risk – as has been called for recently [9–11] – are matters of much interest and the development of new methods to monitor adducts in human DNA may advance our understanding of these roles.

Liquid chromatography coupled with electrospray ionization tandem mass spectrometry (LC/ESI-MS/MS) is a powerful technique that allows for sensitive DNA adduct detection in the picogram range as low as approximately 1 adduct per to 10^9 bases and through the tandem MS, powerful selectivity options are available by utilizing one stage of mass analysis to preselect an ion of interest and a second stage to analyze the induced fragments. Indeed, the future of LC/ESI-MS/MS as a reliable method for analyzing DNA adducts may have strong potential [12–14]. Exploiting these positive aspects of LC/ESI-MS/MS, various groups have developed methods for measuring different DNA adduct types, from different tissues, and from different organisms [15–19] for example and reviewed in [13]. Additionally, multiple DNA adduct monitoring by LC/ESI-MS/MS or by other techniques has also been conducted in some circumstances and sometimes with the aim to compare correlations between different adduct types and/or tissue types [20–23].

The development of techniques that allow for simultaneous monitoring of multiple types of DNA adducts that are complementary to DNA adduct identification processes shall expand our capabilities to analyze DNA damage across a wide spectrum of potential experimental designs. These may include the examination of differences among individuals based upon variables such as occupational exposure, lifestyle, age, sex and genotype. Specifically, comparisons may be performed by analyzing DNA from the same organs of different individuals for example, or comparisons may be performed by analyzing DNA obtained from different locations within the same tissue, or from among different tissues but from within the same individual for example. Currently, although the number of studies may be limited, examination of intratissue and intertissue variations to DNA damage susceptibility may provide insights on a number of issues related to DNA adduct formation in humans. Examples include the capability to compare the relative repair potential or cell turnover of a specific tissue with adduct formation, or the capability to determine the specific susceptibilities of different tissue types or regions of tissue to specific types of DNA damage. In this report, an assessment of intertissue DNA adduct variation from peripherally- and centrally-located lung tissue and esophagus tissue obtained from the same individual is presented and the potential of the adductome approach [24] is discussed.

2. Materials and methods

2.1. Biochemicals and chemicals

The enzymes micrococcal nuclease (MN) and bovine spleen phosphodiesterase II (SPD) were purchased from Worthington Biochemical Corp., (Lakewood, NJ, USA). Bacterial alkaline phosphatase Type III (*E. coli*) and calf thymus DNA were purchased from Sigma Co., (St. Louis, MO, USA). Acrolein monomer was purchased from Tokyo Chemical Industry Co., Ltd. (TCI, Tokyo, Japan) and [U-$^{15}N_5$]-2′-deoxyguanosine ([U-$^{15}N_5$]-dG, 98% purity) was from Cambridge Isotope Laboratories, Inc., Andover, MA, USA.

Analytical standards of the following DNA adducts, N^2-ethyl-2′-deoxyguanosine (N^2-ethyl-dG), the stereoisomers α-*S*- and α-*R*-methyl-γ-hydroxy-1,N^2-propano-2′-deoxyguanosine (1,N^2-PdG$_1$, 1,N^2-PdG$_2$), 3-(2′-deoxyribosyl)-5,6,7,8-tetrahydro-8-hydroxy-pyrimido[1,2-*a*]purine-(3*H*)-one (8-OH-PdG) and the two stereoisomers 3-(2′-deoxyribosyl)-5,6,7,8-tetrahydro-6-hydroxypyrimido[1,2-*a*]purine-(3*H*)-one (6-OH-PdG) were synthesized as described below, while standards of 1,N^6-etheno-2′-deoxyadenosine (εdA) and dideoxyinosine (ddI) were purchased from Sigma. Acetaldehyde (AA), formaldehyde, *trans*-2-butenal (crotonaldehyde), sodium cyanoborohydride ($NaBH_3CN$), dimethyl sulfoxide (DMSO) and methanol, HPLC grade, were purchased from Wako Chemical (Osaka, Japan).

2.2. Preparation of DNA adduct internal standards

Preparation of 2′-deoxyguanosine-acrolein adducts, 6-OH-PdG and 8-OH-PdG, was carried out by reacting 10 mg of 2′-deoxyguanosine with 6 μl of acrolein in 12 ml of 0.025 M phosphate buffer (pH 7.5). The incubation proceeded for five days in the dark in a 37 °C water bath with reciprocal shaking at 150 rpm. The resulting reaction mixture was subjected to reverse phase column chromatography by application to Sep-Pak C18 cartridges (Waters Corp., Milford, MA, USA) whereby the columns were preconditioned with 10 ml methanol and 5 ml distilled water, and the sample was applied and eluted with approximately 5 ml of methanol. The result-

ing solutions were each concentrated en vacuo, recombined and redissolved in a total of 600 μl of DMSO. Fifty microliter aliquots of sample were subjected to preparative HPLC using a Shimadzu LC10-ATVP model pump (Shimadzu, Kyoto, Japan) equipped with a Rheodyne model 7725i injector (Rheodyne, Cotati, CA, USA) and a C18 reverse phase column (Shim-pack FC-ODS, 150 mm × 4.6 mm, Shimadzu) and the fractions were collected. The mobile phase consisted of a water and methanol gradient, whereby water was increased to 40% over a period of 40 min at a flow rate of 1 ml/min. [U-$^{15}N_5$]-6-OH-PdG and [U-$^{15}N_5$]-8-OH-PdG were prepared in the same manner as their unlabeled counterparts, but on a smaller scale by reacting 100 μg of [U-$^{15}N_5$]-dG with 2 μl of acrolein in 400 μl of 0.025 M phosphate buffer.

[U-$^{15}N_5$]-N^2-ethyl-dG was prepared using a modification of a previous method [25] by reacting 100 μl of AA with a 1 mg/ml solution of [U-$^{15}N_5$]-dG in a total reaction volume of 1 ml at 37 °C in the dark for 12 h. Afterwards, $NaBH_3CN$, approximately 20 mg, was added to the mixture in 30 min intervals over a period of 2 h while the reaction was continued at 37 °C. The resulting solution was subjected to reverse phase column chromatography as described in the clean-up of the acrolein reaction products, vacuum concentrated, redissolved in 200 μl of DMSO and purified also as described above. [U-$^{15}N_5$]-1,N^2-PdG$_1$ and [U-$^{15}N_5$]-1,N^2-PdG$_2$ were prepared by adding 20 μl of crotonaldehyde to 1 ml of [U-$^{15}N_5$]-dG (1 mg/ml) for a reaction time of 12 h at 37 °C and [U-$^{15}N_5$]-εdA was synthesized from [U-$^{15}N_5$]-dA according to a previously published method [26]. Purification of the diastereomers [U-$^{15}N_5$]-1,N^2-PdG$_1$ and [U-$^{15}N_5$]-1,N^2-PdG$_1$, and [U-$^{15}N_5$]-εdA was carried out in the same manner as described in the preparation of [U-$^{15}N_5$]-N^2-ethyl-dG. Unlabeled authentic standards of N^2-ethyl-dG, 1,N^2-PdG$_1$ and 1,N^2-PdG$_2$ were prepared in the same manner as described for each, but with unlabeled deoxyguanosine. Purities of all adduct standards were confirmed by measuring absorbance in a GeneSpec V ultraviolet (UV)–vis spectrophotometer with accompanying software (Hitachi Naka Instruments, Co., Ltd., Tokyo, Japan) and the quantity of each purified standard was measured.

2.3. Esophagus and lung tissue DNA extraction and digestion

Human lung and esophagus tissue were obtained postmortem from a Japanese female aged 78 years and were stored in ethanol at −80 °C until DNA purification. DNA was purified with the Puregene DNA Purification System (Gentra Systems, Minneapolis, MN, USA) according to the manufacturer's instructions and desferroxamine was included in the extraction solutions (final concentration 0.1 mM). DNA was obtained from (1) centrally-located lung tissue, from the region of the right middle lobar bronchus bifurcation, (2) peripherally-located lung tissue, from the distal edge of the right inferior lobe and (3) esophagus tissue, obtained mid-region, approximately equidistant from the pharynx and the cardia. Purified DNA was suspended in 500 μl of distilled water and quantification was carried out by measuring absorbance at 260 and 280 nm in a 50 μl volume quartz cell with a UV–vis spectrophotometer. Based upon DNA concentration, aliquots containing 100 μg of DNA were transferred to 1.5 ml Eppendorf tubes and subjected to vacuum concentration (model CC-105 centrifugal concentrator, Tomy Seiko Co., Tokyo, Japan). Following water removal, lung DNA samples were enzymatically hydrolyzed to their corresponding 2′-deoxyribonucleoside-3′-monophosphates by the addition of 100 μl of MN/SPD buffer (200 mM citrate buffer, 100 mM $CaCl_2$, pH 6.0), plus 10 μl each of MN (15 U/μl) and SPD (0.05 U/μl). Solutions were gently mixed by hand and incubated for 2 h at 37 °C. After incubation, 30 units of alkaline phosphatase, 100 μl of 0.5 M Tris–HCl (pH 8.5), 50 μl of 20 mM $ZnSO_4$ and 700 μl of distilled water were added. The solution was again gently mixed and incubated further for 3 h at 37 °C. After incubation the sample volume was reduced to approximately 40 μl by centrifugal concentration and the tube contents were extracted twice with chilled methanol. To each tube, 300 μl of methanol were added, the tubes were shaken for approximately 3 min at 2500 rpm on an Eyela model CM-100 mixer (Tokyo, Japan) and followed by centrifugation at 15,000 × g at 4 °C for 5 min in a Tomy MTX-150 refrigerated centrifuge (Tomy Seiko Co.). The supernatant extract was removed to a new tube, and the pellet was extracted again with methanol and combined with the previous methanol extract for a total volume of 600 μl. Lastly, the methanol was removed by centrifugal concentration and the remaining 2′-deoxynucleosides were resuspended in 1 ml of a 2 ng/ml solution of ddI internal standard in distilled water. In addition to the esophagus and lung tissue DNA, unreacted calf thymus DNA, 100 μg, was treated in an identical manner prior to LC/ESI-MS/MS analyses.

2.4. Instrumentation

LC/ESI-MS/MS analyses were performed using a Shimadzu HPLC system (Shimadzu) consisting of dual LC-10ADVP pumps and equipped with an SPD-10ADVP UV–vis detector interfaced with a Quattro Ultima triple stage quadrupole mass spectrometer (Micromass, Manchester, UK). The LC column was eluted over a gradient that began at a ratio of 15% methanol to 85% water and was changed to 80% methanol to 20% water over a period of 10 min. The 80:20 conditions were held for 10 min and then returned to the original starting conditions, 15:85, which was held for the remaining 8 min. The total run time was 28 min during which the sample components were delivered to the mass spectrometer by electrospray. Sample injection volumes of 50 μl each were injected by a Shimadzu SIL-10ADVP autoinjector, separated on a Shim-pack FC-ODS, 150 mm × 4.6 mm column (Shimadzu) and eluted at a flow rate of 0.5 ml/min. Mass spectral analyses were carried out in positive ion mode with nitrogen as the nebulizing gas. The ion source temperature was 130 °C, the desolvation temperature was 380 °C, and the cone voltage was operated at a constant 35 V. Nitrogen gas was also used as the desolvation gas (700 l/h) and

cone gas (35 l/h) and argon was used as the collision gas at a collision cell pressure of 1.5×10^{-3} mBar. Positive ions were acquired in MRM mode and the strategy was designed to detect the neutral loss of 2′-deoxyribose from positively ionized 2′-deoxynucleoside adducts by monitoring the samples transmitting their $[M+H]^+ > [M+H-116]^+$ transitions. For each tissue DNA sample, from centrally- and peripherally-located lung tissue and esophagus tissue DNA, 374 MRM transitions were monitored over the *m/z* range from transition *m/z* 228.8 > 112.8 through transition *m/z* 602.8 > 486.8. For each 50 μl sample injection (5 μg of digested DNA on column), a total of 32 channels were monitored simultaneously, with one channel for each injection reserved to monitor the ddI internal standard at transition *m/z* 236.8 > 136.8. By using this strategy, each sample was injected 12 times to complete the monitoring of transitions from *m/z* 228.8 to 602.8.

The unambiguous identification of specific target adducts N^2-ethyl-dG, εdA, 1,N^2-PdG$_1$, 1,N^2-PdG$_2$, 8-OH-PdG and two isomers of 6-OH-PdG was performed by comparison to authentic adduct standards and by stable isotope dilution under the same LC/ESI-MS/MS conditions as explained above except that the flow rate was 0.4 ml/min and the mobile phase was 98% water and 2% methanol, increased linearly to 60% water and 40% methanol for 40 min, further increased to 20% water and 80% methanol for 5 min and then returned to the original starting conditions of 98% water and 2% methanol for a total run time of 60 min. MRM transitions for each adduct type were monitored as follows: [U-$^{15}N_5$]-1,N^2-PdG$_1$, [U-$^{15}N_5$]-1,N^2-PdG$_2$, *m/z* 342.8 > 226.8; 1,N^2-PdG$_1$, 1,N^2-PdG$_2$, *m/z* 337.8 > 221.8; [U-$^{15}N_5$]-6-OH-PdG, [U-$^{15}N_5$]-8-OH-PdG, 329.0 > 213.0; 6-OH-PdG, 8-OH-PdG, 324.0 > 208.0; [U-$^{15}N_5$]-N^2-ethyl-dG, *m/z* 300.9 > 184.9; N^2-ethyl-dG *m/z* 295.9 > 179.9; [U-$^{15}N_5$]-εdA, *m/z* 280.9 > 164.9; εdA, *m/z* 275.9 > 159.9.

2.5. Data processing

Data processing was performed in stages as described previously [24]. First putative DNA adduct peaks were integrated using MassLynx 4.0 Global Mass-Informatics Software, secondly, peak integration data were transferred to a spreadsheet and normalized based upon the quantity of ddI internal standard detected for each injection, thirdly, manual screening for 2′-deoxynucleoside artifacts was carried out as summarized in Table 1. In the final stage of data processing, chromatograms for each $[M+H]^+ > [M+H-116]^+$ transition, from *m/z* 228.8 to 602.8, were analyzed to identify and eliminate DNA adduct "ghost" isotope peaks and data were organized to produce the adductome maps. In the final analysis, bubble-type charts were created whereby the LC column retention time of the putative adduct is indicated on the *x*-axis, the mass to charge ratio of the putative adduct is indicated on the *y*-axis, and the bubble size represents the putative adduct peak integration area normalized by the internal standard peak integration area, and is referred to as the area response.

Table 1
Positively ionized 2′-deoxynucleoside artifacts

Base[a]	$+H^+$	$+NH_4^+$	$+Na^+$	$+K^+$	Dimer + H^+
dC	228.09	245.09	250.09	266.09	455.18
dT	243.09	260.09	265.09	281.09	485.09
dA	252.10	269.10	274.10	290.10	503.20
dG	268.10	285.10	290.10	306.10	535.20
5-Methyl-dC	242.11	259.11	264.11	280.11	483.11

Values are given as *m/z*.
[a] 2′-Deoxycytidine; 2′-deoxythymidine; 2′-deoxyadenosine; 2′-deoxyguanosine.

3. Results and discussion

3.1. Adductome maps of lung, esophagus and calf thymus negative control

Figs. 1 and 2 graphically represent the final analyses for centrally- and peripherally-located lung tissue DNA samples (Fig. 1A and 1B respectively), for esophagus tissue DNA (Fig. 2A) and for negative control calf thymus DNA (Fig. 2B) all organized as adduc-

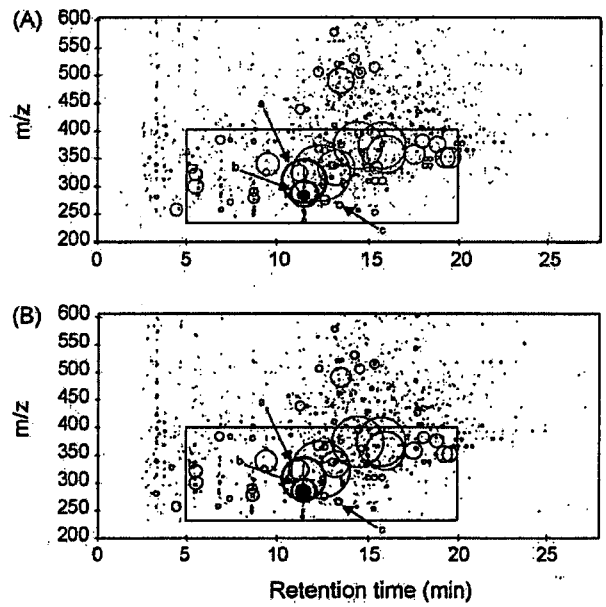

Fig. 1. Two adductome maps of putative DNA adducts detected in central (A) and peripheral (B) human lung tissue DNA from the same individual. The neutral loss of 2′-deoxyribose from positively ionized 2′-deoxynucleoside putative adducts was analyzed by LC/ESI-MS/MS in MRM mode transmitting the $[M+H]^+ > [M+H-116]^+$ transition over a total of 374 transitions in the mass range from *m/z* 228.8 to 602.8. The active zone is indicated by the box and putative adducts *a* through *c* are labeled in the figure and discussed in the text. The blackened bubble (referred to as putative adduct *d* in the text) indicates a putative adduct that was detected at high levels in the DNA of both lung tissue samples but that was detected at a level more than two orders of magnitude lower in esophagus tissue DNA.

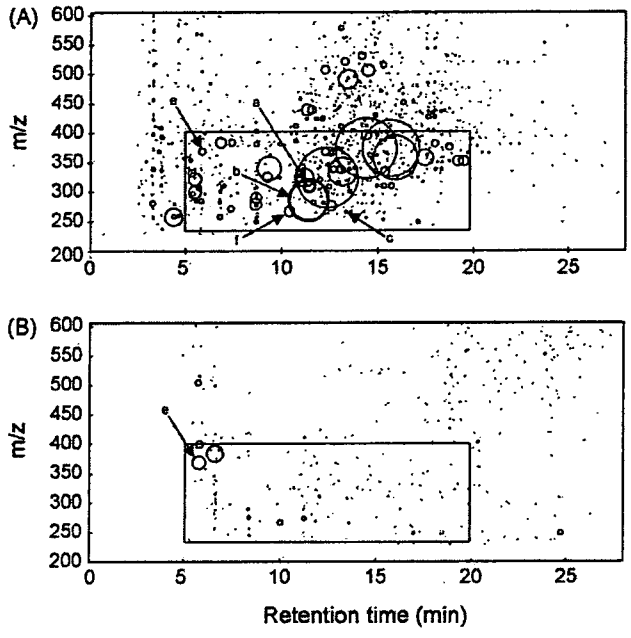

Fig. 2. Adductome maps of putative DNA adducts detected in human esophagus tissue DNA (A) and negative control calf thymus DNA (B). The active zone is indicated by the box and putative adducts *a* through *f* are labeled in the figure and discussed in the text.

tome maps. Putative DNA adducts were more or less detected over the entire *m/z* range in all cases and based upon the observed putative adduct bubble sizes and pattern formations in each adductome map, a high degree of similarity among the two lung tissue DNA samples and the esophagus tissue DNA sample was revealed (Fig. 1A and B and Fig. 2A). These results are in strong contrast to the adductome map of a negative control produced as a result of DNA digestion, LC/ESI-MS/MS analysis and data processing of calf thymus DNA (Fig. 2B).

In lung and esophagus tissue DNA samples, adductome mapping revealed that the most abundant putative adducts occurred similarly in many cases and with similar area response values, but clear differences were also revealed. In all three samples, the highest zone of activity was detected between 5 and 20 min for putative adducts that possessed *m/z* values approximately less than 400 and this zone is indicated in Figs. 1 and 2 by the rectangular box. This active zone, defined by large numbers of putative adducts that possessed the highest area response values, is similar to that which was shown to occur previously in lung tissue DNA taken from a smoker and non-smoker [24]. However, when these data are compared to previous adductome analyses of lung tissue DNA, the most abundant putative adducts detected in this study were markedly different compared to the most abundant putative adducts detected prior, and in addition, these new putative adducts possessed area response values that were up to two orders of magnitude greater than the most abundant putative adducts detected before. Considering these limited data sets, for now it may simply be concluded that such differences reflect the exposure profiles and metabolism of the individuals from whom the DNA was obtained. Of particular interest in regard to the above situation was that the seven most abundant putative adducts detected in lung in the previous study [24] were also detected in the two lung adductome analyses performed in this study. Additionally, a comparison of the average area response values of the putative adducts from these two separate studies indicated that the average area response values did not differ by any order of magnitude, but were in fact found to be quite similar as shown in Table 2. For this analysis, the most abundant putative adducts in the previous study were defined whereby at least one putative adduct of a putative adduct pair possessed an area response value greater than 10; seven putative adducts qualified. Indeed, as indicated in Table 2, after matching putative adducts from the two different studies by retention time and *m/z*, the similarities between the average area response values of previously analyzed lung tissue DNA samples and lung tissue DNA samples from this study ranged from almost equal to approximately only six times different (in one case, *m/z* 323.8) and no differences occurred by an order of magnitude. These data indicate that these putative adducts may be relatively conserved at these levels in lung tissue and may lend support to data set validation by indicating that the most abundant putative adducts detected in this study were a result of a more specific exposure or circumstances. Of course, further adductome analyses of lung tissue DNA samples are necessary and as such analyses are performed, a clearer pattern may emerge.

3.2. Comparison of putative adducts

From all three tissue DNA samples, the 50 most abundant adducts, based upon area response, were aligned by *m/z* and retention time and compared ($n = 50$). The two lung samples shared 90% similarity, while esophagus DNA was 84 and 80% similar to peripheral lung DNA and central lung DNA respectively. The area response values of the most abundant 50 putative adducts represented approximately 85% of the total area response values of all putative adducts detected in each of the three samples ($85.6 \pm 0.4\%$, $n = 3$) while the largest 20, 30 and 100 putative adducts represented approximately the 76th, 81st and 90th percentiles respectively with little standard deviation among the three samples: 76.8 ± 0.8,

Table 2
Similarity of the average area response values of the most abundant putative adducts in lung tissue DNA from a previous study ($n=7$) and the corresponding identical putative adducts observed in lung tissue DNA in this study

m/z	Lung tissue DNA from previous study[a]		Lung tissue DNA from this study	
	R/T (min)[b]	Area response[c]	*R/T* (min)	Area response
257.8	4.43–4.47	24.9 ± 0.5	4.41–4.43	28.7 ± 7.3
278.8	8.68–8.72	17.6 ± 4.3	8.66–8.73	31.0 ± 5.2
283.8	11.46–11.50	51.1 ± 15.9	11.44–11.48	25.6 ± 1.6
289.8	8.68–8.70	17.2 ± 2.8	8.64–8.73	20.7 ± 3.4
323.8	11.25–11.27	12.2 ± 4.9	11.19–11.23	74.2 ± 13.0
337.8	13.08–13.12	12.1 ± 7.9	13.10	13.7 ± 0.7
383.8	6.89–6.91	25.5 ± 3.0	6.81–6.87	18.9 ± 0.2

[a] Kanaly et al. [24].
[b] LC retention time, based upon putative adduct peak height maxima and indicated as a range. In one instance where the putative adduct peak maxima were identical, no range is indicated.
[c] Average area response values of lung DNA putative adduct pairs with the range indicated. The area response value is equal to the putative DNA adduct LC chromatogram peak integration area normalized by the internal standard LC chromatogram peak integration area, ddI.

81.3 ± 0.7 and 90.0 ± 0.3% respectively, $n=3$ in each case. Considering that over 1000 putative adducts were detected in each of the three tissue samples, and that the most abundant 20–100 putative adducts represented 76–90% of the total number of adducts by area response value, it seems prudent to focus our investigative attention on these putative adducts which occur in the most abundant 20–100 putative adducts at this time in the early development of the technique. Study continuation with multiple samples from the same tissues of the same individual and coupled with comparisons to other individuals shall increase our understanding in regard to the range of intratissue, intertissue and interindividual DNA adduct variation.

3.3. *Intertissue variation revealed by the final analyses*

By organizing the final analyses as adductome maps, similarities and some differences were revealed between the three tissue samples. In Fig. 1, attention is drawn to the presence of four putative adducts that were detected with relatively similar area response values in the active zone of the two lung DNA samples. These four unidentified putative adducts are designated in the adductome maps by letters *a* through *c* with a fourth putative adduct bubble blackened for the purpose of reducing any confusion in regard to the putative adduct designations and is hereafter referred to as putative adduct *d*. As mentioned, these four putative adducts: (*a*) *m/z* 307.8, *R/T* 11.46–11.48 (where *R/T* is retention time); (*b*) *m/z* 285.8, *R/T* 11.48; (*c*) *m/z* 265.8, *R/T* 13.36–13.40 and (*d*) *m/z* 283.8, *R/T* 11.44–11.48 all possessed relatively similar area response values in lung tissue but were found to be different when compared to esophagus tissue (Fig. 2A). Although the reasons for these differences are not clear now, such differences may represent differential DNA adduct susceptibility between the lungs and esophagus. For example, putative adduct *a* was detected at nearly equal high levels in both lung tissue DNA samples (area response = 388.4 ± 13.8; difference = ±3.6%) but was more than an order of magnitude lower in esophagus DNA (area response = 27.3; approximately 14 times lower). As shown in Figs. 1 and 2 Figs. 1A, 1B and 2A, although putative adduct *b* was detected at relatively high levels in all three samples – the average area response value was equal to 131.0 ± 17.8 in lung tissue DNA – it was detected at more than twice that level in esophagus tissue DNA (area response = 296.0). Adductome mapping also revealed that putative adducts *c* and *d* occurred to larger extents and at relatively equal levels in lung tissue DNA but occurred to a lesser extent (putative adduct *c*) or did not appear at all in the adductome map of esophagus tissue DNA (putative adduct *d*). The utility of representing the final analyses as adductome maps for comparing intertissue variation is adequately illustrated in the case of putative adduct *d*. Map comparisons (Figs. 1 and 2) clearly indicate the similarities and differences among the four DNA samples. After attention was drawn to putative adduct *d*, it was later determined that it was indeed detected in esophagus tissue DNA but to an extent that was too small to appear in maps of this scale. The area response value of putative adduct *d* in esophagus tissue DNA was 0.14, a level that was more than two orders of magnitude lower than that detected in lung tissue DNA.

Additionally, adductome mapping revealed at least two cases whereby putative adducts were detected at rel-

atively high levels in esophagus tissue DNA (Fig. 2A) but not in lung tissue DNA (Fig. 1A and B). As shown in Fig. 2A, putative adducts *e* and *f* were detected in esophagus tissue DNA (area response values = 11.3 and 21.8 respectively) but were detected at greater than 7- and 10-fold lower levels in lung tissue DNA (average area response values = 1.6 ± 0.1 and 1.9 ± 0.1 respectively) and did not appear in the adductome maps from lung tissue DNA. As shown in the adductome map in Fig. 2B, putative adduct *e* was detected at the highest level overall in calf thymus DNA, area response equal to 35.1, which was three times higher than the level detected in esophagus tissue DNA. Clearly indicated in Fig. 2B was that application of the adductome mapping technique to calf thymus DNA revealed low numbers of adducts that possessed high area response values. Although these data lend support to the validity of the technique, more sample analyses are required, including the assessment of other DNA samples that may serve as appropriate negative controls. For example, salmon testes, human placenta and bacterial DNA have been useful for this purpose in the past [16].

3.4. Unambiguous adduct identification in tissue samples and assignment of adduct identities in adductome maps

Fig. 3 shows identical areas of an expansion of the active zone of the adductome maps created for central lung tissue DNA and esophagus tissue DNA in Figs. 1A and 2A respectively. The retention time ranges from 5 to 20 min and the mass to charge ratio ranges from *m/z* 250 to 375 in these expansion charts. Indeed, included in this *m/z* range and retention time range are all putative adducts previously discussed in Figs. 1 and 2 and they are indicated in Fig. 3 for reference. Noteworthy are that the presence of putative adducts *e* and *f* were revealed in lung tissue DNA by this expansion, but that the level of putative adduct *d* was still too low to be detected. Indeed, the area response value of putative adduct *d* differed by more than order of magnitude from putative adducts *e* and *f*.

A major issue for expanding the power of the final analyses and validating the adductome mapping technique is the unambiguous assignment of identities to the putative adducts that appear in the maps. This process is paramount to the usefulness of the technique in the future. Considering this, four DNA adduct standards, 1,N^2-PdG$_1$, 1,N^2-PdG$_2$, N^2-ethyl-dG and εdA, and their [U-^{15}N$_5$]-stable isotope analogues were synthesized and used to assay for the presence of these adducts in lung tissue and esophagus tissue DNA by LC/ESI-MS/MS.

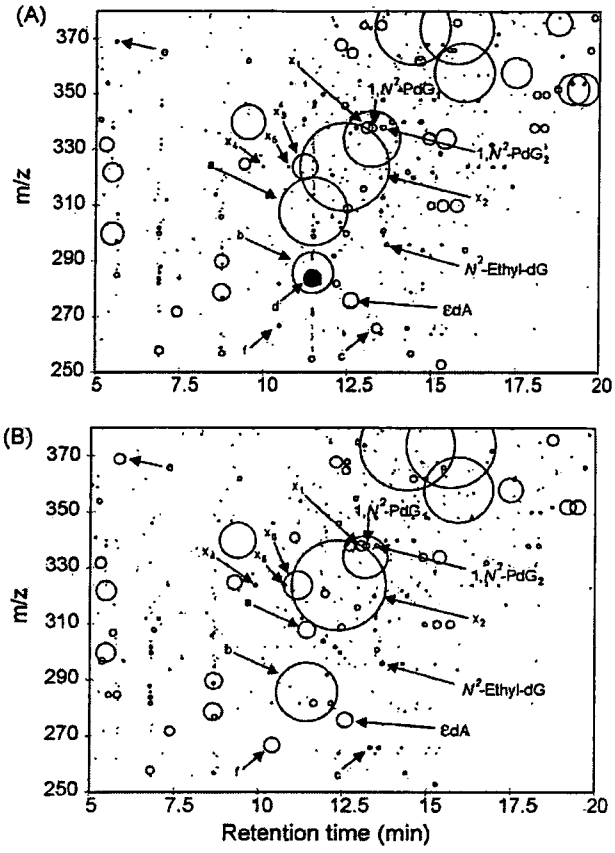

Fig. 3. Expansion of identical areas of the active zone from central lung tissue DNA (A) and esophagus tissue DNA (B) taken from the adductome maps in Figs. 1A and 2A. The exact positions of four DNA adducts whose identities were initially confirmed: 1,N^2-PdG$_1$, 1,N^2-PdG$_2$, N^2-ethyl-dG and εdA are indicated directly in the figure. They were identified by comparison to authentic standards and by radioisotope dilution LC-ESI/MS/MS. Putative adducts x_1 through x_5 and putative adducts *a* through *f* are indicated in the figure and discussed in detail in the text.

These adducts were unambiguously detected in all three tissue DNA samples and their exact positions in the adductome maps were determined as indicated in Fig. 3. Identification of each adduct was made by comparison to authentic standards using an identical LC elution gradient as used for adductome map analyses (as shown for 1,N^2-PdG$_1$ and 1,N^2-PdG$_2$ in lung tissue DNA in Fig. 4A and B for example) and in conjunction with unambiguous identification by spiking of [U-^{15}N$_5$]-stable isotope standards into lung tissue and esophagus tissue samples post-digestion followed by LC/ESI-MS/MS re-analysis utilizing higher resolution LC conditions (as shown for εdA in lung tissue DNA in Fig. 4C and D for example). Based upon our understanding that the most abundant 100 putative adducts detected in this study represented 90% of the number of putative adducts by area response

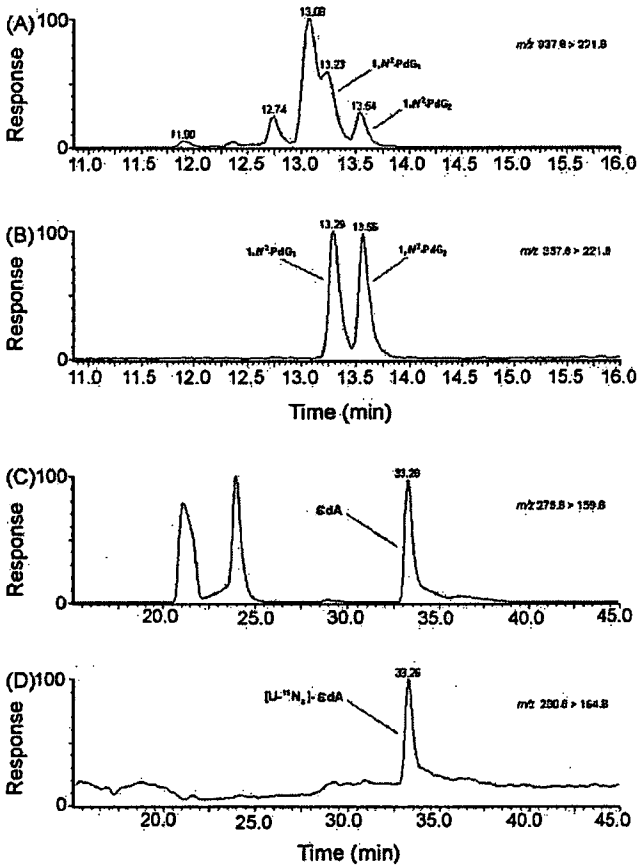

Fig. 4. LC/ESI-MS/MS detection of adducts in DNA obtained from centrally-located human lung tissue by comparison to authentic standards and by stable isotope dilution. (A) Lung tissue sample DNA compared to (B) 1,N^2-PdG$_1$ and 1,N^2-PdG$_2$ authentic standards (*m/z* 337.8 > 221.8); (C) lung tissue DNA (*m/z* 275.8 > 159.8) compared to (D) [U-$^{15}N_5$]-εdA (*m/z* 280.8 > 164.8). The LC retention times are indicated above the peaks in minutes.

in these samples, it was notable that three of the four positively identified adducts fell into this range. εdA was detected with relatively high area response values overall and represented the 20th most abundant adduct detected in esophagus tissue for example. N^2-ethyl-dG was the exception and did not occur within the most abundant 100 putative adducts for any sample, but was detected within the most abundant 150 putative adducts in all three cases. Identification of adduct map positions contributes to our overall view of the adductome maps and represents the beginning of the process of attaching identities to putative adducts revealed by the adductome mapping technique. Clearly, the adductome maps revealed the presence of many unidentified abundant putative adducts over a wide molecular weight range and it shall be a challenge to either attach identities to these putative adducts or re-adjust the final analyses based upon the results of future research.

3.5. Refining the process of adductome map creation

In addition to putative adducts *a* through *f* and the unambiguously identified adducts discussed above, five further putative adduct designations (x_1 through x_5) are indicated in the adductome maps in Fig. 3. Putative adduct x_1 (*m/z* 337.8) was revealed in a previous study to be one of the most abundant putative adducts in the lung tissue DNA of a smoker [24]. Based upon its mass to charge ratio it was hypothesized that it might be 1,N^2-PdG$_1$ or 1,N^2-PdG$_2$. Synthesis of stable isotopes of 1,N^2-PdG$_1$ and 1,N^2-PdG$_2$ followed by stable isotope dilution analyses showed that this was not to be the case although 1,N^2-PdG$_1$ and 1,N^2-PdG$_2$ were identified in the sample. When putative adduct x_1 was analyzed under higher resolution LC conditions, five smaller peaks were further resolved to elute with x_1 and based upon the literature it was discussed that these peaks may have represented isomers of the DNA adducts of 1,N^2-propano-dG [24]. In this study, this putative adduct was detected again in lung and esophagus tissues samples except that the area response values for each putative adduct x_1 were all more than half of the value encountered for the smoker in the previous study.

The most abundant putative adduct in both lung tissue samples as indicated in the adductome maps in Figs. 1–3 was putative adduct x_2 which possessed an *m/z* value of 323.8, retention time range of 12.39–12.41 and an area response value equal to 681.8 ± 11.9. In esophagus tissue DNA, putative adduct x_2 occurred similarly and was the second most abundant putative adduct; retention time = 12.39, area response = 686.7. Due to its large area response value, the identity of this putative adduct was checked by synthesizing and purifying three DNA adduct standards of acrolein (8-OH-PdG and two isomers of 6-OH-PdG) which all possess molecular weights of approximately 323. Acrolein was reacted with dG and the ^{15}N-stable isotope analogue of dG as explained in the Section 2, HPLC profiles similar to that shown to occur in previous studies were observed [27,28] and reaction products were purified as 8-OH-PdG and the two stereosiomers of 6-OH-PdG. Utilization of these acrolein-derived DNA adduct standards in further LC/ESI-MS/MS analyses allowed for the identification of these adducts in all three tissue samples and their locations were identified on the adductome maps in Fig. 3A and B; large putative adduct x_3 was identified as 8-OH-PdG and putative adducts x_4 and x_5 were identified as stereoisomers of 6-OH-PdG. Although these analyses confirmed the presence of acrolein-derived adducts in the three samples, the identity of putative adduct x_2

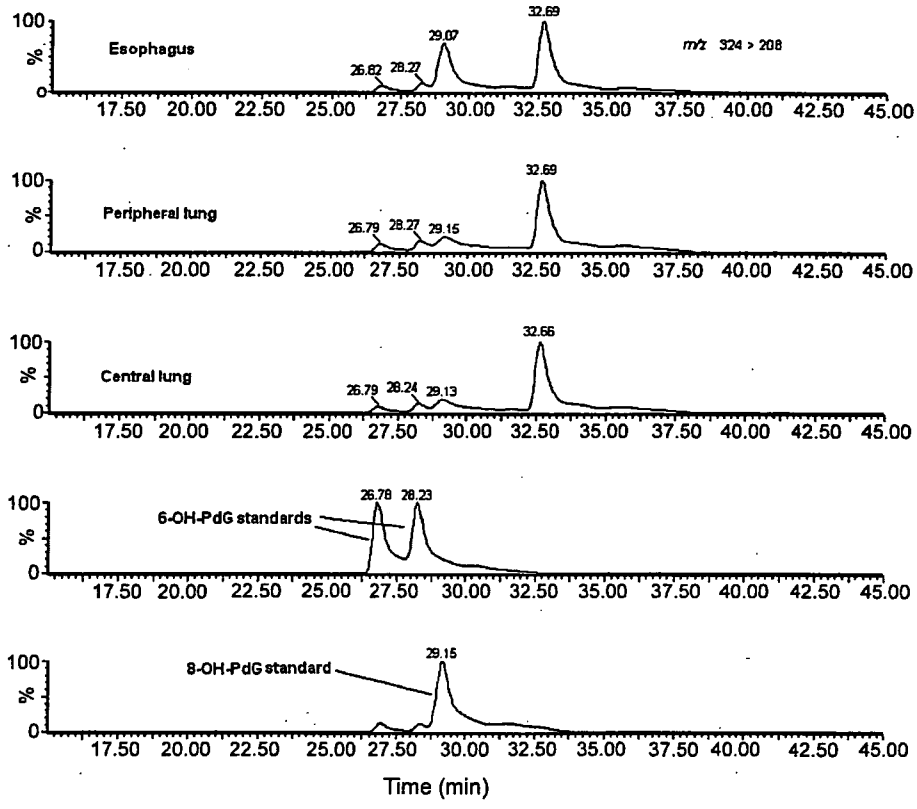

Fig. 5. 6-OH-PdG and 8-OH-PdG adduct detection by LC/ESI-MS/MS in human lung and esophagus tissue DNA by comparison to authentic standards of 6-OH-PdG and 8-OH-PdG (*m/z* 324 > 208). The LC retention times are indicated above the peaks in minutes.

remained unknown. Fig. 5 shows the confirmation of 6-OH-PdG and 8-OH-PdG in all lung and esophagus tissue DNA samples by comparison to authentic 6-OH-PdG and 8-OH-PdG standards.

Overall, a total of seven DNA adducts, N^2-ethyl-dG plus six potentially endogenously- and/or exogenously-produced oxidative adducts, 1,N^2-PdG$_1$, 1,N^2-PdG$_2$, εdA, 8-OH-PdG, and two isomers of 6-OH-PdG were unambiguously detected in all tissue DNA samples in this study and their positions in the adductome maps were located. Indeed, all of these adducts have been detected in humans in different studies and at various levels before [22,29–31]. Exposure to bifunctional electrophilic enals (α,β-unsaturated aldehydes) such as acrolein and crotonaldehyde, through cigarette smoke for example, or through endogenous metabolism via lipid peroxidation may result in the propano adducts identified in this study. Through DNA exposure to exogenous chemicals like urethane, or if enals are converted to more DNA-reactive epoxyaldehydes through cellular oxidative processes, etheno adducts such as εdA may result [1]. Additionally, exposure to acetaldehyde from the environment or through alcohol or tobacco consumption may result in the formation of N^2-ethyl-dG adducts [32].

3.6. Conclusions

Application of the adductome approach for the assessment of intertissue DNA adduct variation was presented for the first time. Assessment of human lung and esophagus tissue DNA revealed many similarities and some distinct differences in the types and abundances of putative adducts detected in the three tissue DNA samples. This assessment demonstrated the utility of the adductome mapping technique by facilitating the visualization of putative adduct detection patterns and their relative levels of occurrence. Application of the adductome approach to calf thymus DNA as a negative control revealed that few putative adducts occurred with high area response values and provided further validation of the technique when compared to tissue DNA samples.

Through the mapping technique, clear similarities and clear differences between the tissue samples were revealed and these allowed for further exploration of those putative adducts of interest. Putative adducts in lung tissue DNA were shown to be 90% similar by this technique while putative adducts in esophagus tissue DNA were shown to be only 80 and 84% similar to central and peripheral lung tissue DNA respectively.

Although over 1000 putative adducts were detected in each of the three tissue DNA samples, analysis indicated that the largest-occurring 100 putative adducts represented 90% of all putative adducts detected in each sample. Unambiguous identification of seven DNA adducts by comparison to authentic adduct standards and stable isotope dilution was performed for all three samples and DNA adduct identities were attached to putative adducts detected by the adductome mapping technique. In terms of technique feasibility, further refinement shall be required such that (1) LC peak resolution is confirmed as adequate, (2) the time required per sample injection is reasonable for the processing of high numbers of samples, (3) data analyses can be completed in a manageable period of time and (4) further validation of reproducibility in terms of adduct type detection and adduct abundance are resolved. Indeed, the attainment of a more appropriate balance of these variables represents one of the challenges in refining the adductome approach for analyzing large numbers of samples.

In closing, the creation of adductome maps from different tissue DNA samples facilitated the visualization of putative DNA adducts and allowed for comprehensive comparisons between samples that would otherwise prove to be difficult. As we continue to assign identities to the putative adducts that are revealed by this methodology, tissue-specific or exposure-specific patterns may continue to emerge and provide further insight on DNA adduct formation in humans.

Acknowledgements

This work was supported in part by grants-in-aid for cancer research from the Japanese Ministry of Health, Labor and Welfare, for scientific research (15681002) from MEXT, Japan, from NEDO, Japan and by the Japan Society for the Promotion of Science (JSPS). We thank Dr. Kentaro Misaki, Kyoto University for synthesizing [U-$^{15}N_5$]-εdA.

References

[1] R. De Bont, N. van Larebeke, Endogenous DNA damage in humans: a review of quantitative data, Mutagenesis 19 (2004) 169–185.
[2] G.N. Wogan, S.S. Hecht, J.S. Felton, A.H. Conney, L.A. Loeb, Environmental and chemical carcinogenesis, Semin. Cancer Biol. 14 (2004) 473–486.
[3] S. Bjelland, E. Seeberg, Mutagenicity, toxicity and repair of DNA base damage induced by oxidation, Mutat. Res. 531 (2003) 37–80.
[4] M.S. Cooke, M.D. Evans, M. Dizdaroglu, J. Lunec, Oxidative DNA damage: mechanisms, mutation, and disease, FASEB J. 17 (2003) 1195–1214.
[5] M.S. Cooke, R. Olinski, M.D. Evans, Does measurement of oxidative damage to DNA have clinical significance? Clin. Chim. Acta 365 (2005) 30–49.
[6] L.J. Marnett, J.N. Riggins, J.D. West, Endogenous generation of reactive oxidants and electrophiles and their reactions with DNA and protein, J. Clin. Invest. 111 (2003) 583–593.
[7] W.L. Neeley, J.M. Essigmann, Mechanisms of formation, genotoxicity, and mutation of guanine oxidation products, Chem. Res. Toxicol. 19 (2006) 491–505.
[8] G. Slupphaug, B. Kavli, H.E. Krokan, The interacting pathways for prevention and repair of oxidative DNA damage, Mutat. Res. 531 (2003) 231–251.
[9] D.H. Phillips, DNA adducts as markers of exposure and risk, Mutat. Res. 577 (2005) 284–292.
[10] R.M. Santella, M. Gammon, M. Terry, R. Senie, J. Shen, D. Kennedy, M. Agrawal, B. Faraglia, F.-F. Zhang, Mutat. Res. 592 (2005) 29–35.
[11] A. Rundle, Carcinogen-DNA adducts as a biomarker for cancer risk, Mutat. Res. 600 (2006) 23–36.
[12] P.B. Farmer, K. Brown, E. Tompkins, V.L. Emms, D.J.L. Jones, R. Singh, D.H. Phillips, DNA adducts: mass spectrometry methods and future prospects, Toxicol. Appl. Pharmacol. 207 (2005) 293–301.
[13] H. Koc, J.A. Swenberg, Applications of mass spectrometry for quantitation of DNA adducts, J. Chromatogr. B 778 (2002) 323–343.
[14] R. Singh, P.B. Farmer, Liquid chromatography-electrospray ionization-mass spectrometry: the future of DNA adduct detection, Carcinogenesis 27 (2006) 178–196.
[15] F.A. Beland, M.I. Churchwell, L.S. Von Tungeln, S. Chen, P.P. Fu, S.J. Culp, B. Schoket, E. Gyorffy, J. Minárovits, M.C. Poirier, E.D. Bowman, A. Weston, D.R. Doerge, High-performance liquid chromatography electrospray ionization tandem mass spectrometry for the detection and quantitation of benzo[a]pyrene-DNA adducts, Chem. Res. Toxicol. 18 (2005) 1306–1315.
[16] D.R. Doerge, M.I. Churchwell, J.-L. Fang, F.A. Beland, Quantification of etheno-DNA adducts using liquid chromatography, on-line sample processing, and electrospray tandem mass spectrometry, Chem. Res. Toxicol. 13 (2000) 1259–1264.
[17] X. Liu, M.A. Lovell, B.C. Lynn, Detection and quantification of endogenous cyclic DNA adducts derived from trans-4-hydroxy-2-nonenal in human brain tissue by isotope dilution capillary liquid chromatography nanoelectrospray tandem mass spectrometry, Chem. Res. Toxicol. 19 (2006) 710–718.
[18] E.M. Ricicki, J.R. Soglia, C. Teitel, R. Kane, F. Kadlubar, P. Vouros, Detection and quantification of *N*-(deoxyguanosin-8-yl)-4-aminobiphenyl adducts in human pancreas tissue using capillary liquid chromatography-microelectrospray mass spectrometry, Chem. Res. Toxicol. 18 (2005) 692–699.
[19] N.M. Thomson, R.S. Mijal, R. Ziegel, N.L. Fleischer, A.E. Pegg, N.Y. Tretyakova, L.A. Peterson, Development of a quantitative liquid chromatrography/electrospray mass spectrometric assay for a mutagenic tobacco specific nitrosamine-derived DNA adduct, O^6-[4-oxo-4-(3-pyridyl)butyl]-2′-deoxyguanosine, Chem. Res. Toxicol. 17 (2004) 1600–1606.
[20] M.I. Churchwell, F.A. Beland, D.A. Doerge, Quantification of multiple DNA adducts formed through oxidative stress using liquid chromatography and electrospray tandem mass spectrometry, Chem. Res. Toxicol. 15 (2002) 1295–1301.
[21] A. Barbin, H. Ohgaki, J. Nakamura, M. Kurrer, P. Kleihues, J.A. Swenberg, Endogenous deoxyribonucleic acid (DNA) damage in human tissues: a comparison of ethenobases with aldehydic

DNA lesions. Cancer Epidemiol. Biomarkers Prev. 12 (2003) 1241–1247.
[22] R. Godschalk, J. Nair, F.J. van Schooten, A. Risch, P. Drings, K. Kayser, H. Dienemann, H. Bartsch, Comparison of multiple DNA adduct types in tumor adjacent human lung tissue: effect of cigarette smoking, Carcinogenesis 23 (2002) 2081–2086.
[23] F.F. Kadlubar, K.E. Anderson, S. Häussermann, N.P. Lang, G.W. Barone, P.A. Thompson, S.L. MacLeod, M.W. Chou, M. Mikhailova, J. Plastaras, L.J. Marnett, J. Nair, I. Velic, H. Bartsch, Comparison of DNA adduct levels associated with oxidative stress in human pancreas, Mutat. Res. 405 (1998) 125–133.
[24] R.A. Kanaly, T. Hanaoka, H. Sugimura, H. Toda, S. Matsui, T. Matsuda, Development of the adductome approach to detect DNA damage in humans, Antoxid. Redox Signal. 8 (2006) 993–1001.
[25] M. Sako, H. Kawada, K. Hirota, A convenient method for the preparation of N^2-ethylguanine nucleosides and nucleotides, J. Org. Chem. 64 (1999) 5719–5721.
[26] P. Raboisson, A. Baurand, J.-P. Cazenave, C. Gachet, M. Retat, B. Spiess, J.-J. Bourguignon, Novel antagonists acting at the P2Y1 purigenic receptor: synthesis and conformational analysis using potentiometric and nuclear magnetic resonance titration techniques, J. Med. Chem. 45 (2002) 962–972.
[27] G. Cheng, Y. Shi, S.J. Sturla, J.R. Jalas, E.J. McIntee, P.W. Villalta, M. Wang, S.S. Hecht, Reactions of formaldehyde plus acetaldehyde with deoxyguanosine and DNA: formation of cyclic deoxyguanosine adducts and formaldehyde cross-links, Chem. Res. Toxicol. 16 (2003) 145–152.
[28] X. Liu, M.A. Lovell, B.C. Lynn, Development of a method for quantification of acrolein-deoxyguanosine adducts in DNA using isotope dilution-capillary LC/MS/MS and its application to human brain tissue, Anal. Chem. 77 (2005) 5982–5989.
[29] J.-L. Fang, C.E. Vaca, Detection of DNA adducts of acetaldehyde in peripheral white blood cells of alcohol abusers, Carcinogenesis 18 (1997) 627–632.
[30] R.G. Nath, F.-L. Chung, Detection of exocyclic 1,N^2-propanodeoxyguanosine adducts as common DNA lesions in rodents and humans, Proc. Natl. Acad. Sci. USA 91 (1994) 7491–7495.
[31] R.G. Nath, J.E. Ocando, J.B. Guttenplan, F.-L. Chung, 1,N^2-Propanodeoxyguanosine adducts: potential new biomarkers of smoking-induced DNA damage in human oral tissue, Cancer Res. 58 (1998) 581–584.
[32] D. Pluskota-Karwatka, A.J. Pawowicz, L. Kronberg, Formation of malonaldehyde-acetaldehyde conjugate adducts in calf thymus DNA, Chem. Res. Toxicol. 19 (2006) 921–926.

Available online at www.sciencedirect.com
ScienceDirect
Mutation Research 633 (2007) 46–54
Genetic Toxicology and Environmental Mutagenesis
www.elsevier.com/locate/gentox
Community address: www.elsevier.com/locate/mutres

Detection of oxidative DNA damage, cell proliferation and *in vivo* mutagenicity induced by dicyclanil, a non-genotoxic carcinogen, using *gpt* delta mice

Takashi Umemura [a,*], Yuichi Kuroiwa [a], Masako Tasaki [a], Toshiya Okamura [a], Yuji Ishii [a], Yukio Kodama [b], Takehiko Nohmi [c], Kunitoshi Mitsumori [d], Akiyoshi Nishikawa [a], Masao Hirose [a]

[a] *Divisions of Pathology, National Institute of Health Sciences, 1-18-1, Kamiyoga, Setagaya-ku, Tokyo 158-8501, Japan*
[b] *Divisions of Toxicology, National Institute of Health Sciences, 1-18-1, Kamiyoga, Setagaya-ku, Tokyo 158-8501, Japan*
[c] *Divisions of Genetics and Mutagenesis, National Institute of Health Sciences, 1-18-1, Kamiyoga, Setagaya-ku, Tokyo 158-8501, Japan*
[d] *Laborartory of Veterinary Pathology, Tokyo University of Agriculture and Technology, 3-5-8, Saiwai-cho, Fuchu-shi, Tokyo 183-8509, Japan*

Received 10 April 2007; received in revised form 9 May 2007; accepted 10 May 2007
Available online 18 May 2007

Abstract

To ascertain whether measurement of possible contributing factors to carcinogenesis concurrently with the transgenic mutation assay is useful to understand the mode of action underlying tumorigenesis of non-genotoxic carcinogens, male and female *gpt* delta mice were given dicyclanil (DC), a mouse hepatocarcinogen showing all negative results in various genotoxicity tests, at a carcinogenic dose for 13 weeks. Together with *gpt* and Spi$^-$ mutations, thiobarbituric acid-reactive substances (TBARS), 8-hydroxydeoxyguanosine (8-OHdG) and bromodeoxyuridine labeling indices (BrdU-LIs) in the livers were examined. Whereas there were no changes in TBARS levels among the groups, significant increases in 8-OHdG levels and centrilobular hepatocyte hypertrophy were observed in the treated mice of both genders. In contrast, BrdU-LIs and liver weights for the treated females, but not the males were significantly higher than those for the controls. Likewise, the *gpt* mutant frequencies (MFs) in the treated females were significantly elevated, GC:TA transversion mutations being predominant. No significant alterations were found in the *gpt* MFs of the males and the Spi$^-$ MFs of both sexes. The results for the transgenic mutation assays were consistent with DC carcinogenicity in terms of the sex specificity for females. Considering that 8-OHdG induces GC:TA transversion mutations by mispairing with A bases, it is likely that cells with high proliferation rates and a large amounts of 8-OHdG come to harbor mutations at high incidence. This is the first report demonstrating DC-induced genotoxicity, the results implying that examination of carcinogenic parameters concomitantly with reporter gene mutation assays is able to provide crucial information to comprehend the underlying mechanisms of so-called non-genotoxic carcinogenicity.

Keywords: 8-Hydroxydeoxyguanosine; Cell proliferation; *gpt* delta mice; Dicyclanil

1. Introduction

The standard battery of genotoxicity tests consisting of an *in vitro* test for gene mutations in bacteria, an *in vitro* test for chromosomal damage and/or gene

* Corresponding author. Tel.: +81 3 3700 1141; fax: +81 3 3700 1425.
E-mail address: umemura@nihs.go.jp (T. Umemura).

1383-5718/$ – see front matter © 2007 Elsevier B.V. All rights reserved.
doi:10.1016/j.mrgentox.2007.05.007

mutations in mammalian cells and an *in vivo* test for chromosomal damage in rodent hematopoietic cells is usually applied in order to identify genotoxicity of environmental chemicals such as pesticides, food additives and pharmaceuticals [1]. However, the existence of discrepancies between genotoxicity and *in vivo* long-term carcinogenicity is well known [2]. There are several reasons which may explain the occurrence of false negative or positive results. For instance, although most carcinogens require biotransformation to DNA reactive species for the purpose of exerting genotoxic effects, the enzyme systems to metabolize xenobiotics in both bacteria and mammalian cells using *in vitro* assays are lacking or are expressed to only a limited extent [3]. Likewise, in *in vivo* short-term assays, it is doubtful whether target cells are exposed to test chemicals at adequate doses for a sufficient period of time, partly because of test chemical toxicity and/or a low biotransformation capacity in hematopoietic cells [3]. Thus, it is a natural consequence that alternative batteries of *in vitro* and/or *in vivo* genotoxicity tests do not fully make up the gap [4], which means we must focus our attention on the mode of action in terms of the risk assessment for environmental agents.

In this respect, reporter gene-transgenic rodents may be useful tools to predict carcinogenicity because studies can be performed with similar protocols as for the long-term bioassay [5]. Transgenic mutation assays also have the advantage of allowing a battery of other *in vivo* mutation assays such as micronucleus tests in the same animals [6]. Additionally, various proposed mechanisms underlying the actions of direct genotoxic carcinogens (e g. generation of DNA adducts) [7], indirect genotoxic carcinogens (e.g. aneugenicity or oxidative DNA damage) [8] and non-genotoxic carcinogens (e.g. methylation, mitogenicity or cytotoxicity-associated cell proliferation) [9–11] are able to be investigated concurrently with transgenic mutation assays. In fact, we have reported that simultaneous analysis of glutathione *S*-transferase placental form (GST-P) immunohistochemistry in the livers of *gpt* delta rats provided crucial information for understanding the chemical carcinogenesis of 2-amino-3-methylimidazo[4,5-*f*]quinoline, *N*-nitrosopyrrolidine and di(2-ethylhexyl)phthalate [12]. Also, finding of increases in hepatocyte proliferation together with a lack of the transgene mutations in *gpt* delta mice given flumequine, an anti-bacterial quinolone agent, helped us to define this mouse liver carcinogen as a genuine promoter [13].

Dicyclanil (4,6-diamino-2-cyclopropylaminopyrimidine-5-carbonaitrite; DC), a pyrimidine-derived insect growth regulator, has given all negative results for *in vitro* reverse mutations, gene mutations, chromosomal aberrations, unscheduled DNA synthesis, *in vivo* micronucleus formation [14] and alkaline single cell electrophoretic change [15]. However, DC has been reported to be a hepatocarcinogen in female mice [14] and recent studies revealed a possible involvement of oxidative stress [16]. In the present study, to explore the mode of action underlying DC hepatocarcinogenesis, lipid peroxidation, 8-hydroxydeoxyguanosine (8-OHdG) and hepatocyte proliferation in the livers of male and female *gpt* delta rats given DC at a carcinogenic dose were examined along with the transgenic mutation assay.

2. Materials and methods

2.1. Chemicals

Dicyclanil was kindly provided by Novartis Animal Health Co., Ltd. (Basel, Switzerland) (Fig. 1). Alkaline phosphatase and bromodeoxyuridine (BrdU) were obtained from Sigma Chemical Co. (St. Louis, MO, USA) and nuclease P1 from Yamasa Co. (Chiba, Japan).

2.2. Animals and treatments

The protocol for this study was approved by the Animal Care and Utilization Committee of the National Institute of Health Sciences. Male and female B6C3F1 *gpt* delta mice carrying 80 tandem copies of the transgene lambda EG10 in a haploid genome status were raised by mating of C57BL/6 *gpt* delta and non-transgenic C3H/He mice (Japan SLC, Inc., Shizuoka, Japan). Ten male and 10 female B6C3F1 *gpt* delta mice were each randomized by weight into two groups. They were housed in a room with a barrier system, and maintained under the following constant conditions: temperature of 23 ± 2 °C, relative humidity of 55 ± 5%, ventilation frequency of 18 times/h and a 12-h light:12-h dark cycle, with free access to CRF-1 basal diet (Oriental Yeast Co., Ltd., Tokyo, Japan) and tap water. Starting at 8 weeks of age the mice were

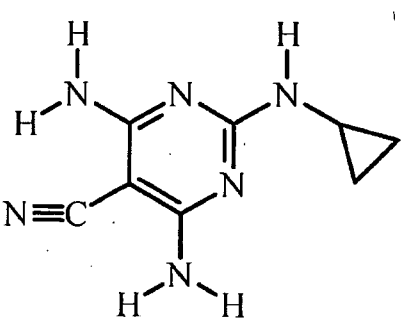

Fig. 1. Chemical structure of dicyclanil (DC).

fed diet containing 0.15% DC or maintained as non-treatment controls for 13 weeks. The dose of DC was a reported carcinogenic dose in a 18-month carcinogenicity study [14]. All mice received BrdU (100 mg/kg) by i.p. injection once a day for the final 2 days of exposure and once on the final day, 2 h before killing, as previous described [17]. All mice were killed at week 13 by exsanguination under ether anesthesia and the livers were immediately removed and weighed; slices were fixed in buffered formalin for hematoxylin and eosin (H&E) staining or BrdU immunohistochemistry. Remaining pieces of liver were frozen with liquid nitrogen and stored at −80 °C until measurement of 8-OHdG in nuclear DNA, and levels of thiobarbituric acid-reactive substances (TBARS) and performance of mutation assays.

2.3. Measurement of nuclear 8-OHdG

In order to prevent 8-OHdG formation as a byproduct during DNA isolation [18], liver DNA was extracted by a slight modification of the method of Nakae et al. [19]. Briefly, nuclear DNA was extracted with a commercially available DNA Extracter WB Kit (Wako Pure Chemical Industries, Ltd., Osaka, Japan) containing an antioxidant NaI solution to dissolve cellular components. For further prevention of autooxidation in the cell lysis step, deferoxamine mesylate (Sigma Chemical Co.) was added to the lysis buffer [20]. DNA was digested to deoxynucleotides with nuclease P1 and alkaline phosphatase and levels of 8-OHdG (8-OHdG/10^5 deoxyguanosine) were assessed by high-performance liquid chromatography (HPLC) with an electrochemical detection system (Coulochem II, ESA, Bedford, MA, U.S.A.).

2.4. Measurement of TBARS

Malondialdehyde (MDA, nmol/g) was assessed as an index of lipid peroxidation by the method of Uchiyama and Mihara [21]. In brief, a 0.15 g portion of liver was homogenized with 1.35 mL of 1.15% KCl solution. To 0.05 mL of this homogenate, 0.2 mL 8.1% SDS and 3.0 mL 0.4% 2-thiobarbituric acid in 10% acetic acid solution (pH 3.5) were added, followed by heating in a water bath at 95 °C for 60 min. After cooling, 5.0 mL of *n*-butanol and pyridine (15:1, v/v) and 1.0 mL distilled water were added and the mixture was centrifuged at 1870 × *g* for 10 min. TBARS were measured with a Hitachi F-2500 fluorescence spectrophotometer (Hitachi High-Technologies Co., Tokyo, Japan) at 515 nm (excitation) and 553 nm (emission) in the butanol/pyridine phase.

2.5. Immunohistochemical procedures

For immunohistochemical staining of BrdU, sections were treated sequentially with normal horse serum, monoclonal mouse anti-BrdU (1:80), biotin-labeled horse anti-mouse IgG (1:400) and avidin–biotin–peroxidase complex (ABC) after denaturation of DNA with 4N HCl. The sites of peroxidase binding were demonstrated by incubation with 3,3′-diaminobenzidine tetrahydrochloride (Sigma Chemical Co.). The immunostained sections were lightly counterstained with hematoxylin for microscopic examination.

2.6. Cell proliferation quantification

For each animal at least 3000 hepatocytes were counted. The labeling index (BrdU-LI) was calculated as a percentage value derived from the number of labeled cells divided by the total number of cells counted.

2.7. In vivo mutation assays

6-TG and Spi$^-$ selections were performed as previously described [5]. Briefly, genomic DNA was extracted from the livers, and lambda EG10 DNA (48 kb) was rescued as the lambda phage by *in vitro* packaging. For 6-TG selection, the packaged phage was incubated with *Escherichia coli* YG6020, which expresses Cre recombinase, and converted to a plasmid carrying *gpt* and chloramphenicol acetyltransferase. Infected cells were mixed with molten soft agar and poured onto agar plates containing chloramphenicol and 6-TG. In order to determine the total number of rescued plasmids, 3000-fold diluted phages were used to infect YG6020, and poured on the plates containing chloramphenicol without 6-TG. The plates were then incubated at 37 °C for selection of 6-TG-resistant colonies. Positively selected colonies were counted on day 3 and collected on day 4. The mutant frequency (MF) was calculated by dividing the number of *gpt* mutants by the number of rescued phages.

For the Spi$^-$ selection, the packaged phage was incubated with *E. coli* XL-1 Blue MRA for survival titration and *E. coli* XL-1 Blue MRA P2 for mutant selection. Infected cells were mixed with molten lambda-trypticase agar plates. Next day, plaques (Spi$^-$ candidates) were punched out with sterilized glass pipetters and the agar plugs were suspended in SM buffer. In order to confirm the Spi$^-$ phenotype of candidates, the suspensions were spotted on three types of plates where XL-1 Blue MRA, XL-1 Blue MRA P2 or WL95 P2 strains were spread with soft agar. Real Spi$^-$ mutants, which made clear plaques on every plate, were counted.

For characterizing the mutation spectra of *gpt* mutants, a 739 bp DNA fragment containing the 456 bp coding region of the *gpt* gene was amplified by PCR as described previously [5]. DNA sequencing was performed with Big Dye™ Terminater Cycle Sequencing Ready Reaction (Applied Biosystems, Foster City, CA, USA) on an ABI PRISM™ 310 Genetic Analyzer (Applied Biosystems).

2.8. Statistical evaluation

For statistical analysis, the Student's *t*-test was used to compare body and liver weights, as well as quantitative data for BrdU-LIs, TBARS, 8-OHdG and MFs between groups.